UCRL-TR-201913

LAWRENCE LIVERMORE NATIONAL LABORATORY

Estimated (n,f) cross sections for ^{236,236m,237,238}Np, ^{237,237m}Pu, and ^{240,241,242,242m,243,244,244m}Am isotopes

W. Younes, H.C. Britt, and J.A. Becker

January 16, 2004

This document was prepared as an account of work sponsored by an agency of the United States Government. Neither the United States Government nor the University of California nor any of their employees, makes any warranty, express or implied, or assumes any legal liability or responsibility for the accuracy, completeness, or usefulness of any information, apparatus, product, or process disclosed, or represents that its use would not infringe privately owned rights. Reference herein to any specific commercial product, process, or service by trade name, trademark, manufacturer, or otherwise, does not necessarily constitute or imply its endorsement, recommendation, or favoring by the United States Government or the University of California. The views and opinions of authors expressed herein do not necessarily state or reflect those of the United States Government or the University of California, and shall not be used for advertising or product endorsement purposes.

Estimated (n, f) cross sections for ^{236,236m,237,238}Np, ^{237,237m}Pu, and ^{240,241,242,242m,243,244,244m}Am isotopes

W. Younes,* H. C. Britt, and J. A. Becker

Lawrence Livermore National Laboratory, Livermore, CA 94551

(Dated: January 16, 2004)

Abstract

Neutron-induced fission cross sections on targets of ^{236,236m,237,238}Np, ^{237,237m}Pu, and ^{240,241,242,242m,243,244,244m}Am have been estimated for incident neutron energies of up to 6 MeV, using the "surrogate" technique and the $(^3\text{He}, df)$ and $(^3\text{He}, tf)$ reactions on stable targets to measure fission probabilities. In isotopes where low-lying isomeric states are known to exist, the (n, f) cross section on the corresponding isomeric targets has been estimated, using the surrogate technique. For targets of ^{237}Np, ^{241}Am, ^{242m}Am, and ^{243}Am, measurements of the (n, f) cross section exist, and comparison with the surrogate-method results suggests that the (n, f) cross sections estimated by the surrogate technique are reliable to within 10% for incident neutron energies $E_n \gtrsim 2$ MeV. Tabulated values of the estimated (n, f) cross sections are given in an appendix.

*Electronic address: `younes@llnl.gov`

I. INTRODUCTION

In a previous report [1] we summarized results on estimated (n, f), hard-to-measure cross sections for a series of U and Pu isotopes in the energy range 0.1 to 2.5 MeV, obtained from the analysis of (t, pf) reaction results. In the surrogate technique, (n, f) cross sections are obtained by combining fission probabilities measured in direct-reaction, fission-correlation experiments with calculated neutron compound nucleus formation cross sections, and a correction for the difference in transferred spin and parity distributions. From a comparison of these cross sections to directly measured cross sections for nuclei where such measurements exist, it was estimated that the overall reliability of this indirect technique is approximately $\pm$ 10% for incident neutron energies $E_n \gtrsim 1$ MeV, equal to the estimated systematic uncertainties for fission probabilities quoted by the authors for the original (t, pf) experiment [2].

In the present work we have extended the surrogate technique to the analysis of similar fission probability data sets measured for a series of actinide targets at the Los Alamos National Laboratory in the mid 1970s [3], using the reactions $(^3\mathrm{He}, df)$ and $(^3\mathrm{He}, tf)$. A previous attempt to estimate neutron cross sections for these data sets was published in 1979 [4]. In the previous work, (1) an empirically estimated cross section of 3.1 barns was used for the neutron compound nucleus formation cross section and (2) no corrections were made for the difference in angular momentum distributions for the ^{3}He reactions relative to the neutron capture reaction. In the present work we have improved the reliability of the model by (1) utilizing newly-calculated neutron compound nucleus cross sections [5–7], and (2) by extending our angular-momentum-dependent analysis to include the ^{3}He reactions.

We present results for (n, f) cross sections from $E_n = 0.1$ to 6 MeV for 6 ground state nuclei and 3 isomers that cannot be directly measured. Four of the nuclei studied here (^{236}Np, ^{237}Pu, ^{242}Am, and ^{244}Am) contain long lived isomers where the isomer and ground state cross sections are predicted to differ by up to 20-40% at energies below 1 MeV. For ^{238}Np and ^{240}Am, the surrogate technique provides the only possible experimental data. We also present (n, f) cross sections for 4 test cases (^{237}Np, ^{241}Am, ^{242m}Am, and ^{243}Am) where our estimated (n, f) cross sections can be compared to direct measurements. These cases demonstrate the reliability of our technique and validate the estimated $\pm$ 10% uncertainties assigned to the measured fission probabilities. The list of nuclei studied and their properties are given in Table XIV. The estimated (n, f) cross sections for the actinide targets discussed

in this paper are tabulated in appendix A

II. EXPERIMENTAL DETAILS

The actinide $(^3\mathrm{He}, df)$ and $(^3\mathrm{He}, tf)$ fission-probability data used in this paper are taken from Gavron *et al.* [3]. The fission probabilities were measured as a function of excitation energy in the compound system, following the $(^3\mathrm{He}, d)$ or $(^3\mathrm{He}, t)$ reaction. The outgoing deuteron or triton was identified using a particle telescope situated at 120° with respect to the incident-beam direction. Two fission detectors, situated near forward and backward angles were used to count fission events. The number of detected coincidences between deuterons (or tritons) and fission fragments, divided by the total number of deuterons (or tritons) detected, and corrected for detection efficiency, produces the fission probability. The excitation energy of the fissioning nucleus was reconstructed from the measured energy of the outgoing particle and the kinematics of the reaction.

Corrections of up to 15% were applied to the fission-probability data by Gavron *et al.* [3] to compensate for the presence of a tungsten contaminant in all the targets. The presence of a tungsten contaminant tends to lower the measured fission probabilities by generating extraneous $(^3\mathrm{He}, d)$ and $(^3\mathrm{He}, t)$ events. Systematic errors in the measured fission probabilities are estimated at less than 10%.

III. METHOD

The surrogate technique has been described in detail in Refs. [6, 7]. Only the salient features of model are recalled here.

The $(^3\mathrm{He}, xf)$ reactions (where $x = d$ or t) are treated as a two-step process. The direct $(^3\mathrm{He}, x)$ reaction forms a composite system, which subsequently equilibrates and fissions. Thus the fission probability, calculated as a function of excitation energy in the compound system can be written as the sum

$$P_{(^3\mathrm{He},xf)}(E_\mathrm{x}) = \sum_{J^\pi} P_{(^3\mathrm{He},x)}(J^\pi) \times P_f(E_\mathrm{x}, J^\pi), \tag{1}$$

where the population probabilities $P_{(^3\mathrm{He},x)}(J^\pi)$ following the direct reaction are calculated in a distorted-wave Born approximation approach, and are essentially independent of excitation

energy over the energy range of interest. The fission probabilities $P_f(E_\mathrm{x}, J^\pi)$ are independent of the population mechanism, and are calculated assuming statistical competition between γ decay, neutron emission, and fission. In practice, the $P_f(E_\mathrm{x}, J^\pi)$ probabilities are calculated using a standard double-humped fission model and the fission-barrier heights are adjusted to reproduce the measured probabilities $P_{(^3\mathrm{He},xf)}(E_\mathrm{x})$.

Once the optimal fission probability components $P_f(E_\mathrm{x}, J^\pi)$ have been found, the (n, f) cross section is obtained by folding them with a neutron-compound cross section, σ_{CN}, calculated with the same transmission coefficients used in the description of the neutron-emission channel,

$$\sigma_{(n,f)}(E_n) = \sum_{J^\pi} \sigma_{CN}(E_n, J^\pi) \times P_f(E_\mathrm{x}, J^\pi). \tag{2}$$

The application of these equations improves on earlier work, e.g. by Cramer *et al.* [8] and Britt *et al.* [4], by including the dependence on angular momentum and parity, and by updating the optical-model calculations of the neutron-transmission coefficients, which are required in the expressions for $P_f(E_\mathrm{x}, J^\pi)$ and $\sigma_{CN}(E_n, J^\pi)$ in Eqs. (1) and (2). The neutron compound cross section calculated with the new transmission coefficients is compared in Fig. 1 to the constant 3.1-barn cross section used by Britt *et al.* in their earlier work [4]. The 3.1-barn value is consistent with the new σ_{CN} curve, and can be viewed as an average value of the cross section in the $E_n = 0-8$ MeV range.

In the present calculations, level densities for an even-even nucleus were shifted by neutron and/or proton pairing energies to obtain level densities appropriate for odd-A and odd-odd systems. The pairing energies were obtained by interpolating microscopic-macroscopic calculations [9, 10] of the level densities and pairing energies for the ^{228}Ra, ^{238}U, and ^{248}Cm nuclei. Experimental discrete levels, where available, were used up to the pairing gap energy in the first wells. In the remaining cases, the calculated continuous level densities were used at all excitation energies. Discrete transition states were used on top of the inner and outer barriers for even-even compound nuclei only (i.e., only for the ^{237,237m}Pu neutron targets). In odd-A and odd-odd systems, the calculated continuous level densities were used at all excitation energies. Unlike the previous work [6, 7] on (t, pf) surrogate data, the fission probabilities obtained from the $(^3\mathrm{He}, xf)$ data could be fitted without the need for an additional parallel fission path through a second outer barrier. Therefore, a simple

two-barrier model was used in the present work. The population from both (^{3}He, d) and (^{3}He, t) reactions was obtained using a calculated population probability σ_L for the (^{3}He, d) reaction. However, different combinations of coupled spins were used for the two reactions. The (^{3}He, d) reaction was treated as a one-proton transfer, and the population of a particular spin and parity J^π in the compound system, for a target with given spin I_0 and parity π_0 was taken to be proportional to

$$\sum_{j=|J-I_0|}^{J+I_0} \sum_{L=|j-1/2|}^{j+1/2} \sigma_L \times \delta_{\pi,\pi_0(-1)^L}. \tag{3}$$

The (^{3}He, t), which in principle is a charge-exchange reaction and not a transfer reaction, was assumed to proceed via both total-spin 0 and 1 transfers, and the population probability for particular spin and parity J^π in the compound system was assumed to be proportional to

$$\sum_{j=|J-I_0|}^{J+I_0} \left[\sigma_{L=0} \times \delta_{\pi,\pi_0} + \sum_{L=|j-1|}^{j+1} \sigma_L \times \delta_{\pi,\pi_0(-1)^L} \right]. \tag{4}$$

Neutron transmission coefficients, calculated for the n + ^{241}Pu reaction [5], were used for all the cases studied in this paper. The calculations could be specialized to each reaction, however the variance of the transmission coefficients over the range of nuclei considered in this work is a few percent, at most, and does not have a substantial effect on the results.

IV. RESULTS

A. Comparison of surrogate to directly measured cross sections

In Figs 2-5 we show fission probabilities and (n, f) cross sections for ^{237}Np, ^{241}Am, ^{242m}Am and ^{243}Am. The fission-probability data are reasonably reproduced by the model described in section III. As in the (t, pf) cases [1, 6, 7] the model is only used to generate a correction factor and the surrogate (n, f) cross sections are renormalized to the experimental fission probability values. For the (n, f) cross sections we show for comparison the surrogate results from the present model, earlier surrogate results with an empirical model [4], evaluations

from ENDF/B-VI [11] and ENDL [12] for the ^{237}Np, ^{241}Am, and ^{243}Am targets, and experimental (n, f) data for the ^{242m}Am target.

In Fig. 6, the estimate of the (n, f) cross section, ENDF/B-VI evaluation and selected experimental (n, f) data are compared for the ^{237}Np, ^{241}Am, ^{242m}Am and ^{243}Am targets. In the case of the ^{237}Np, ^{241}Am, and ^{243}Am nuclei, the ENDF/B-VI cross-section curve is fairly representative of the data, although there is some scatter of the data sets, particularly in the case of ^{243}Am. The ENDF/B-VI evaluation of the ^{242m}Am(n, f) cross section is ill-behaved, and we have used the data of Browne *et al.* [13] as a standard for comparison.

The agreement between the surrogate cross sections and the comparison standard is generally very good above 3 MeV for 3 cases (^{237}Np, ^{241}Am compared to ENDF/B-VI, and ^{242m}Am compared to the data of Browne *et al.*). In the ^{242m}Am case, both the data of Browne *et al.* [13], and the more recent results of Fursov *et al.* [14] are in good agreement with our data. It should be remembered that the principal difference between the previous empirical model [4] and our current model is that the earlier estimates relied on a normalization to the measured (n, f) data sets whereas the current model gives an absolute prediction. At neutron energies below 2 MeV the surrogate results appear to be systematically higher by up to 20%. A similar effect was observed in the (t, pf) results reported earlier [1, 6, 7] below about 1 MeV. The origin of this effect is not clear but the rise in the surrogate (n, f) cross sections does seem to mirror some gross structure that appears in the calculated neutron compound cross sections shown in Fig. 1. Overall, the absolute agreement between surrogate and measured cross sections is quite good. The ratio R of surrogate cross section to measured cross section for the 4 cases is given in Table XV.

For ^{243}Am our results are low by about 20% relative to the most recent measurements [15–19] and by even more relative to the older data of Behrens [20]. The reason for the discrepancy in this case is unclear. However, it should be noted that our ^{243}Am results come from ^{244}Pu$(^3$He$, tf)$ data. It was pointed out in the paper of Gavron et al [3] that some targets had normalization corrections up to 15% due to the presence of a W contaminant from the target preparation process. Details of the exact correction for this target are lost but ^{244}Pu was the most difficult target in the series used for the (n, f) cross section estimates presented in this paper because of the rarity of the isotope. Therefore, it is likely that this target had the maximum (order 15%) correction and possible that this correction was underestimated. If this is the case then our predicted (n, f) cross sections for ^{244}Am are likely to be low

also. Other targets (^{236,238}U, ^{237}Np and ^{239,240,242}Pu) used to obtain the rest of the P_f data used in this paper are by comparison relatively easy and should not have had a significant W contamination problem. The W contamination comes from vacuum evaporation at high temperature and close geometry which is necessary if the material is very rare, or very radioactive.

In summary, the first three cases show absolute average deviations from the measured (n, f) results of less than the 10% systematic uncertainties estimated by the authors for the experimental fission probabilities [3] for $E_n \gtrsim 2$ MeV.

B. (n,f) cross sections for nuclei with long lived isomers

Figs 7-10 show results for 4 nuclear isomeric states with relatively long lifetimes.

The ^{237}Pu case is analogous to ^{235}U, which was treated in detail in our earlier reports [1, 6, 7]. Fig. 8 shows the results for cross sections on the $7/2^-$ ground state and the $1/2^+$ isomer. The ratio of these cross sections in Fig. 8b) shows a relative suppression of the $1/2^+$ isomer cross section in the region below 1 MeV. This ratio is similar in magnitude to the results for ^{235}U [6, 7], but with a slightly different shape. The detailed results depend on the discrete level spectra at the fission saddle points, and these level spectra are not very well known. We believe that the order of magnitude ($\sim$ 20%) of the suppression of the isomer cross section, due to the paucity of low-lying 0^- and 1^+ states at the fission saddles [6], is a more robust prediction than the detailed shape of the ratio function.

The other 3 cases, ^{236m}Np, ^{242m}Am and ^{244m}Am are all odd-odd nuclei that contain closely spaced high spin (5^- or 6^-) and low spin levels ($1^\pm$). In all cases the high spin states have the longest lifetimes. In fact, the only direct experimental neutron cross sections available in this group are for the isomer ^{242m}Am which has a half-life of 141 years. In the region below $E_n = 2$ MeV the results show a consistent enhancement of the fission cross section for neutron capture on the high spin state. This effect varies from 20-40%.

This enhancement is due to the difficulty in coupling from the high-spin states populated in the mass A compound system to the low-spin, low-excitation-energy region in the first well of the mass $A - 1$ residual, populated by neutron emission. The result is inhibited neutron emission. Fig. 9 shows sensitivity tests for ^{242}Am, which confirm this conclusion. If the discrete level spectrum from 0 to 1 MeV in the first well is replaced by a continuous level

density, which includes more high-spin states, then the effect goes away. If the continuous level densities at the saddles are replaced by a simulated discrete spectrum then the results are only slightly modified.

For ^{236}Np, very few levels are known experimentally in the first well, and therefore a continuous spectrum was used. The calculations show a very small isomer-to-ground-state ratio. However if levels for ^{242}Am are arbitrarily used, a fission enhancement for the ground state emerges that is similar to the ^{242}Am case. Thus, ^{236}Np would presumably show this enhancement effect if we had access to a realistic set of discrete states in the first well to use in the calculation.

C. (n,f) cross sections for ^{238}Np and ^{240}Am

Figs 11 and 12 show (n, f) cross sections obtained for ^{238}Np and ^{240}Am targets. The half-lives of 2.1 days (^{238}Np) and 51 hours (^{240}Am) make it unlikely that a direct measurement can be performed. The predicted cross sections are slightly higher than those obtained with the previous empirical model [4].

V. SUMMARY

Results are presented for estimated (n, f) cross sections for a series of Np, Pu and Am isotopes in the energy range $E_n = 0-8$ MeV. The results were obtained from $(^3\mathrm{He}, df)$ and $(^3\mathrm{He}, tf)$ fission-probability data, coupled with calculations of the neutron-induced compound cross section, and corrected for the difference in angular-momentum transfer between neutron and ^{3}He reactions. From comparison with measured values, the surrogate results appear to be accurate to within the $\pm$ 10% systematic uncertainties of the original fission probability measurements [3], for $E_n \gtrsim 2$ MeV. However, for neutron energies below about 2 MeV there is evidence that the surrogate cross section values may be high by up to 10-20%. A similar effect is seen in the earlier (t, pf) results [1, 6, 7]. It is unclear whether this apparent overestimate is due to (1) inaccuracies in the calculated neutron compound cross sections, or (2) some deficiency in the fission probability model in the region where discrete states are important, in the first well and at the fission saddles.

Comparison to earlier estimates of the cross sections using an empirical model [4] shows

that the current model gives slightly higher cross section values except for the special case of odd-odd nuclei with very high target spins (e.g. 5^-, 6^-). In these cases there is an enhancement observed in the fission cross section of 20-40% peaked at about 0.8 MeV neutron energy. This enhancement is due to the hindrance of the decay back to the first well for the high spin states populated in the compound nucleus.

VI. ACKNOWLEDGMENTS

This work was performed under the auspices of the U.S. Department of Energy by the University of California, Lawrence Livermore National Laboratory under contract No. W-7405-Eng-48.

APPENDIX A: TABULATED CROSS SECTIONS

The estimated (n, f) cross sections for targets of ^{236,236m,237,238}Np, ^{237,237m}Pu, and ^{240,241,242,242m,243,244,244m}Am are tabulated in this appendix for easy access and use. The measured fission probability as a function of excitation energy and deduced (n, f) cross section as a function of incident energy are given in each case. An estimated 10% systematic uncertainty on the measured fission probabilities is assigned to the deduced cross sections as well.

TABLE I: Measured ^{236}U(^{3}He, df) fission probabilities and the corresponding deduced ^{236}Np(n, f) cross section. A $\pm$10% uncertainty associated with the fission probability data is quoted and reflected in the uncertainty on the deduced $\sigma_{(n,f)}$ values (in barns).

E_x	$P_{(t,pf)}(E_x)$		E_n	$\sigma_{(n,f)}(E_n)$	
(MeV)	Value	Unc.	(MeV)	Value (b)	Unc. (b)
5.210	0.0400	0.0040			
5.400	0.1500	0.0150			
5.590	0.4500	0.0450			
5.770	0.6300	0.0630			

TABLE I: (Continued).

E_x	$P_{(t,pf)}(E_x)$		E_n	$\sigma_{(n,f)}(E_n)$	
(MeV)	Value	Unc.	(MeV)	Value (b)	Unc. (b)
5.960	0.7800	0.0780			
6.140	0.8500	0.0850			
6.330	0.8400	0.0840			
6.520	0.8700	0.0870			
6.700	0.8000	0.0800	0.126	2.9070	0.2907
6.890	0.7600	0.0760	0.316	2.6920	0.2692
7.070	0.7200	0.0720	0.496	2.4783	0.2478
7.260	0.6800	0.0680	0.686	2.2758	0.2276
7.450	0.6900	0.0690	0.876	2.2882	0.2288
7.630	0.6800	0.0680	1.056	2.2681	0.2268
7.820	0.6800	0.0680	1.246	2.2982	0.2298
8.000	0.6300	0.0630	1.426	2.1549	0.2155
8.190	0.6300	0.0630	1.616	2.1675	0.2167
8.360	0.6800	0.0680	1.786	2.3344	0.2334
8.560	0.6000	0.0600	1.986	2.0390	0.2039
8.750	0.6300	0.0630	2.176	2.1094	0.2109
8.940	0.6500	0.0650	2.366	2.1384	0.2138
9.120	0.6200	0.0620	2.546	2.0041	0.2004
9.300	0.5900	0.0590	2.726	1.8742	0.1874
9.490	0.5900	0.0590	2.916	1.8418	0.1842
9.670	0.5700	0.0570	3.096	1.7522	0.1752
9.860	0.5700	0.0570	3.286	1.7264	0.1726
10.040	0.5900	0.0590	3.466	1.7642	0.1764
10.220	0.5500	0.0550	3.646	1.6253	0.1625
10.410	0.5600	0.0560	3.836	1.6361	0.1636
10.590	0.5500	0.0550	4.016	1.5912	0.1591

TABLE I: (Continued).

E_x	$P_{(t,pf)}(E_x)$		E_n	$\sigma_{(n,f)}(E_n)$	
(MeV)	Value	Unc.	(MeV)	Value (b)	Unc. (b)
10.780	0.5500	0.0550	4.206	1.5768	0.1577
10.960	0.5500	0.0550	4.386	1.5616	0.1562

TABLE II: Measured ^{236}U(^{3}He, df) fission probabilities and the corresponding deduced ^{236m}Np(n, f) cross section. A $\pm 10\%$ uncertainty associated with the fission probability data is quoted and reflected in the uncertainty on the deduced $\sigma_{(n,f)}$ values (in barns).

E_x	$P_{(t,pf)}(E_x)$		E_n	$\sigma_{(n,f)}(E_n)$	
(MeV)	Value	Unc.	(MeV)	Value (b)	Unc. (b)
5.210	0.0400	0.0040			
5.400	0.1500	0.0150			
5.590	0.4500	0.0450			
5.770	0.6300	0.0630			
5.960	0.7800	0.0780			
6.140	0.8500	0.0850			
6.330	0.8400	0.0840			
6.520	0.8700	0.0870			
6.700	0.8000	0.0800	0.126	2.7128	0.2713
6.890	0.7600	0.0760	0.316	2.6129	0.2613
7.070	0.7200	0.0720	0.496	2.4163	0.2416
7.260	0.6800	0.0680	0.686	2.2445	0.2245
7.450	0.6900	0.0690	0.876	2.2734	0.2273
7.630	0.6800	0.0680	1.056	2.2664	0.2266
7.820	0.6800	0.0680	1.246	2.3080	0.2308
8.000	0.6300	0.0630	1.426	2.1717	0.2172
8.190	0.6300	0.0630	1.616	2.1889	0.2189
8.360	0.6800	0.0680	1.786	2.3586	0.2359
8.560	0.6000	0.0600	1.986	2.0594	0.2059
8.750	0.6300	0.0630	2.176	2.1309	0.2131
8.940	0.6500	0.0650	2.366	2.1632	0.2163
9.120	0.6200	0.0620	2.546	2.0316	0.2032

TABLE II: (Continued).

E_x	$P_{(t,pf)}(E_x)$		E_n	$\sigma_{(n,f)}(E_n)$	
(MeV)	Value	Unc.	(MeV)	Value (b)	Unc. (b)
9.300	0.5900	0.0590	2.726	1.9039	0.1904
9.490	0.5900	0.0590	2.916	1.8743	0.1874
9.670	0.5700	0.0570	3.096	1.7854	0.1785
9.860	0.5700	0.0570	3.286	1.7606	0.1761
10.040	0.5900	0.0590	3.466	1.8006	0.1801
10.220	0.5500	0.0550	3.646	1.6601	0.1660
10.410	0.5600	0.0560	3.836	1.6723	0.1672
10.590	0.5500	0.0550	4.016	1.6272	0.1627
10.780	0.5500	0.0550	4.206	1.6115	0.1611
10.960	0.5500	0.0550	4.386	1.5978	0.1598

TABLE III: Measured ^{238}U(^{3}He, tf) fission probabilities and the corresponding deduced ^{237}Np(n, f) cross section. A $\pm 10\%$ uncertainty associated with the fission probability data is quoted and reflected in the uncertainty on the deduced $\sigma_{(n,f)}$ values (in barns).

E_x	$P_{(t,pf)}(E_x)$		E_n	$\sigma_{(n,f)}(E_n)$	
(MeV)	Value	Unc.	(MeV)	Value (b)	Unc. (b)
5.870	0.0800	0.0080	0.382	0.2578	0.0258
6.060	0.2400	0.0240	0.572	0.7987	0.0799
6.250	0.4200	0.0420	0.762	1.4119	0.1412
6.440	0.5800	0.0580	0.952	1.9631	0.1963
6.620	0.6000	0.0600	1.132	2.0529	0.2053
6.810	0.5500	0.0550	1.322	1.9093	0.1909
6.910	0.5800	0.0580	1.422	2.0256	0.2026
7.180	0.5600	0.0560	1.692	1.9650	0.1965
7.370	0.5700	0.0570	1.882	1.9862	0.1986
7.560	0.5500	0.0550	2.072	1.8914	0.1891
7.740	0.5800	0.0580	2.252	1.9630	0.1963
7.930	0.5700	0.0570	2.442	1.8939	0.1894
8.110	0.4800	0.0480	2.622	1.5668	0.1567
8.300	0.5000	0.0500	2.812	1.6029	0.1603
8.480	0.5200	0.0520	2.992	1.6406	0.1641
8.670	0.4800	0.0480	3.182	1.4911	0.1491
8.850	0.5200	0.0520	3.362	1.5938	0.1594
9.040	0.5300	0.0530	3.552	1.6036	0.1604
9.220	0.5300	0.0530	3.732	1.5858	0.1586
9.400	0.5500	0.0550	3.912	1.6289	0.1629
9.580	0.4700	0.0470	4.092	1.3791	0.1379
9.760	0.4400	0.0440	4.272	1.2802	0.1280

TABLE III: (Continued).

E_x	$P_{(t,pf)}(E_x)$		E_n	$\sigma_{(n,f)}(E_n)$	
(MeV)	Value	Unc.	(MeV)	Value (b)	Unc. (b)
9.940	0.4600	0.0460	4.452	1.3277	0.1328
10.130	0.5100	0.0510	4.642	1.4609	0.1461
10.310	0.4900	0.0490	4.822	1.3958	0.1396
10.490	0.4800	0.0480	5.002	1.3623	0.1362
10.670	0.4500	0.0450	5.182	1.2747	0.1275
10.850	0.5000	0.0500	5.362	1.4155	0.1415
11.030	0.4900	0.0490	5.542	1.3878	0.1388
11.210	0.4600	0.0460	5.722	1.3044	0.1304
11.390	0.5000	0.0500	5.902	1.4203	0.1420

TABLE IV: Measured ^{238}U(^{3}He, df) fission probabilities and the corresponding deduced ^{238}Np(n, f) cross section. A $\pm$10% uncertainty associated with the fission probability data is quoted and reflected in the uncertainty on the deduced $\sigma_{(n,f)}$ values (in barns).

E_x	$P_{(t,pf)}(E_x)$		E_n	$\sigma_{(n,f)}(E_n)$	
(MeV)	Value	Unc.	(MeV)	Value (b)	Unc. (b)
5.470	0.1000	0.0100			
5.650	0.3100	0.0310			
5.840	0.6000	0.0600			
6.030	0.7400	0.0740			
6.210	0.7900	0.0790			
6.400	0.7900	0.0790	0.183	2.7019	0.2702
6.580	0.6700	0.0670	0.363	2.2523	0.2252
6.770	0.5400	0.0540	0.553	1.7715	0.1772
6.960	0.5000	0.0500	0.743	1.6357	0.1636
7.140	0.4600	0.0460	0.923	1.5149	0.1515
7.330	0.4400	0.0440	1.113	1.4785	0.1479
7.510	0.4000	0.0400	1.293	1.3701	0.1370
7.700	0.4200	0.0420	1.483	1.4606	0.1461
7.890	0.4200	0.0420	1.673	1.4680	0.1468
8.070	0.4300	0.0430	1.853	1.4970	0.1497
8.260	0.4400	0.0440	2.043	1.5146	0.1515
8.450	0.4200	0.0420	2.233	1.4230	0.1423
8.640	0.4100	0.0410	2.423	1.3642	0.1364
8.820	0.4100	0.0410	2.603	1.3404	0.1340
9.010	0.4000	0.0400	2.793	1.2843	0.1284
9.200	0.4200	0.0420	2.983	1.3259	0.1326
9.380	0.4100	0.0410	3.163	1.2752	0.1275

TABLE IV: (Continued).

E_x	$P_{(t,pf)}(E_x)$		E_n	$\sigma_{(n,f)}(E_n)$	
(MeV)	Value	Unc.	(MeV)	Value (b)	Unc. (b)
9.570	0.4100	0.0410	3.353	1.2571	0.1257
9.750	0.4100	0.0410	3.533	1.2417	0.1242
9.940	0.4000	0.0400	3.723	1.1970	0.1197
10.120	0.4100	0.0410	3.903	1.2143	0.1214
10.300	0.3900	0.0390	4.083	1.1443	0.1144
10.490	0.4000	0.0400	4.273	1.1630	0.1163
10.670	0.4000	0.0400	4.453	1.1537	0.1154
10.850	0.4000	0.0400	4.633	1.1453	0.1145
11.030	0.4100	0.0410	4.813	1.1673	0.1167
11.220	0.4000	0.0400	5.003	1.1342	0.1134
11.400	0.3700	0.0370	5.183	1.0471	0.1047

TABLE V: Measured ^{237}Np(^{3}He, df) fission probabilities and the corresponding deduced ^{237}Pu(n, f) cross section. A $\pm 10\%$ uncertainty associated with the fission probability data is quoted and reflected in the uncertainty on the deduced $\sigma_{(n,f)}$ values (in barns).

E_x	$P_{(t,pf)}(E_x)$		E_n	$\sigma_{(n,f)}(E_n)$	
(MeV)	Value	Unc.	(MeV)	Value (b)	Unc. (b)
5.510	0.0900	0.0090			
5.710	0.1800	0.0180			
5.910	0.2700	0.0270			
6.100	0.4600	0.0460			
6.300	0.5600	0.0560			
6.500	0.7600	0.0760			
6.700	0.7000	0.0700			
6.890	0.8600	0.0860			
7.090	0.8500	0.0850			
7.290	1.0000	0.1000	0.289	3.6352	0.3635
7.490	0.8600	0.0860	0.489	3.0243	0.3024
7.680	0.8000	0.0800	0.679	2.8184	0.2818
7.880	0.8500	0.0850	0.879	2.9772	0.2977
8.080	0.8000	0.0800	1.079	2.8002	0.2800
8.280	0.7700	0.0770	1.279	2.7125	0.2712
8.470	0.7900	0.0790	1.469	2.7993	0.2799
8.670	0.7600	0.0760	1.669	2.6908	0.2691
8.870	0.7800	0.0780	1.869	2.7365	0.2737
9.070	0.8200	0.0820	2.069	2.8329	0.2833
9.260	0.7700	0.0770	2.259	2.6128	0.2613
9.460	0.7200	0.0720	2.459	2.3942	0.2394
9.660	0.7800	0.0780	2.659	2.5424	0.2542

TABLE V: (Continued).

E_x	$P_{(t,pf)}(E_x)$		E_n	$\sigma_{(n,f)}(E_n)$	
(MeV)	Value	Unc.	(MeV)	Value (b)	Unc. (b)
9.860	0.7600	0.0760	2.859	2.4308	0.2431
10.050	0.7300	0.0730	3.049	2.2966	0.2297
10.250	0.7200	0.0720	3.249	2.2296	0.2230
10.450	0.7000	0.0700	3.449	2.1370	0.2137
10.650	0.7200	0.0720	3.649	2.1700	0.2170
10.840	0.7300	0.0730	3.839	2.1758	0.2176
11.040	0.6700	0.0670	4.039	1.9762	0.1976
11.240	0.7400	0.0740	4.239	2.1621	0.2162
11.440	0.7100	0.0710	4.439	2.0564	0.2056
11.630	0.7100	0.0710	4.629	2.0410	0.2041
11.830	0.7000	0.0700	4.829	2.0002	0.2000
12.030	0.7300	0.0730	5.029	2.0783	0.2078
12.230	0.7000	0.0700	5.229	1.9896	0.1990
12.420	0.6900	0.0690	5.419	1.9610	0.1961
12.620	0.6800	0.0680	5.619	1.9343	0.1934

TABLE VI: Measured ^{237}Np(^{3}He, df) fission probabilities and the corresponding deduced ^{237m}Pu(n, f) cross section. A $\pm 10\%$ uncertainty associated with the fission probability data is quoted and reflected in the uncertainty on the deduced $\sigma_{(n,f)}$ values (in barns).

E_x	$P_{(t,pf)}(E_x)$		E_n	$\sigma_{(n,f)}(E_n)$	
(MeV)	Value	Unc.	(MeV)	Value (b)	Unc. (b)
5.510	0.0900	0.0090			
5.710	0.1800	0.0180			
5.910	0.2700	0.0270			
6.100	0.4600	0.0460			
6.300	0.5600	0.0560			
6.500	0.7600	0.0760			
6.700	0.7000	0.0700			
6.890	0.8600	0.0860			
7.090	0.8500	0.0850			
7.290	1.0000	0.1000	0.289	2.8604	0.2860
7.490	0.8600	0.0860	0.489	2.3314	0.2331
7.680	0.8000	0.0800	0.679	2.3602	0.2360
7.880	0.8500	0.0850	0.879	2.7814	0.2781
8.080	0.8000	0.0800	1.079	2.7366	0.2737
8.280	0.7700	0.0770	1.279	2.6755	0.2676
8.470	0.7900	0.0790	1.469	2.7735	0.2773
8.670	0.7600	0.0760	1.669	2.6767	0.2677
8.870	0.7800	0.0780	1.869	2.7318	0.2732
9.070	0.8200	0.0820	2.069	2.8356	0.2836
9.260	0.7700	0.0770	2.259	2.6191	0.2619
9.460	0.7200	0.0720	2.459	2.4002	0.2400
9.660	0.7800	0.0780	2.659	2.5458	0.2546

TABLE VI: (Continued).

E_x	$P_{(t,pf)}(E_x)$		E_n	$\sigma_{(n,f)}(E_n)$	
(MeV)	Value	Unc.	(MeV)	Value (b)	Unc. (b)
9.860	0.7600	0.0760	2.859	2.4310	0.2431
10.050	0.7300	0.0730	3.049	2.2964	0.2296
10.250	0.7200	0.0720	3.249	2.2313	0.2231
10.450	0.7000	0.0700	3.449	2.1412	0.2141
10.650	0.7200	0.0720	3.649	2.1762	0.2176
10.840	0.7300	0.0730	3.839	2.1833	0.2183
11.040	0.6700	0.0670	4.039	1.9839	0.1984
11.240	0.7400	0.0740	4.239	2.1718	0.2172
11.440	0.7100	0.0710	4.439	2.0667	0.2067
11.630	0.7100	0.0710	4.629	2.0523	0.2052
11.830	0.7000	0.0700	4.829	2.0119	0.2012
12.030	0.7300	0.0730	5.029	2.0904	0.2090
12.230	0.7000	0.0700	5.229	2.0004	0.2000
12.420	0.6900	0.0690	5.419	1.9704	0.1970
12.620	0.6800	0.0680	5.619	1.9421	0.1942

TABLE VII: Measured ^{240}Pu(^{3}He, df) fission probabilities and the corresponding deduced ^{240}Am(n, f) cross section. A $\pm 10\%$ uncertainty associated with the fission probability data is quoted and reflected in the uncertainty on the deduced $\sigma_{(n,f)}$ values (in barns).

E_x	$P_{(t,pf)}(E_x)$		E_n	$\sigma_{(n,f)}(E_n)$	
(MeV)	Value	Unc.	(MeV)	Value (b)	Unc. (b)
5.330	0.0400	0.0040			
5.520	0.0800	0.0080			
5.700	0.1700	0.0170			
5.890	0.3600	0.0360			
6.070	0.6200	0.0620			
6.250	0.7100	0.0710			
6.440	0.7000	0.0700			
6.620	0.7400	0.0740			
6.810	0.7200	0.0720	0.169	2.5229	0.2523
6.990	0.7200	0.0720	0.349	2.4716	0.2472
7.180	0.7000	0.0700	0.539	2.3421	0.2342
7.370	0.6500	0.0650	0.729	2.1424	0.2142
7.560	0.6300	0.0630	0.919	2.0818	0.2082
7.750	0.6500	0.0650	1.109	2.1783	0.2178
7.940	0.6100	0.0610	1.299	2.0805	0.2080
8.130	0.6100	0.0610	1.489	2.1088	0.2109
8.320	0.6400	0.0640	1.679	2.2234	0.2223
8.510	0.6400	0.0640	1.869	2.2145	0.2215
8.700	0.6400	0.0640	2.059	2.1905	0.2191
8.890	0.6200	0.0620	2.249	2.0900	0.2090
9.080	0.6200	0.0620	2.439	2.0539	0.2054
9.270	0.6200	0.0620	2.629	2.0174	0.2017

TABLE VII: (Continued).

E_x	$P_{(t,pf)}(E_x)$		E_n	$\sigma_{(n,f)}(E_n)$	
(MeV)	Value	Unc.	(MeV)	Value (b)	Unc. (b)
9.460	0.6300	0.0630	2.819	2.0144	0.2014
9.650	0.6100	0.0610	3.009	1.9187	0.1919
9.840	0.6000	0.0600	3.199	1.8589	0.1859
10.020	0.6300	0.0630	3.379	1.9264	0.1926
10.210	0.6100	0.0610	3.569	1.8418	0.1842
10.400	0.6300	0.0630	3.759	1.8803	0.1880
10.590	0.6000	0.0600	3.949	1.7719	0.1772

TABLE VIII: Measured ^{242}Pu(^{3}He, tf) fission probabilities and the corresponding deduced ^{241}Am(n, f) cross section. A $\pm 10\%$ uncertainty associated with the fission probability data is quoted and reflected in the uncertainty on the deduced $\sigma_{(n,f)}$ values (in barns).

E_x	$P_{(t,pf)}(E_x)$		E_n	$\sigma_{(n,f)}(E_n)$	
(MeV)	Value	Unc.	(MeV)	Value (b)	Unc. (b)
6.150	0.0600	0.0060	0.612	0.1830	0.0183
6.340	0.1900	0.0190	0.802	0.5956	0.0596
6.530	0.3700	0.0370	0.992	1.2036	0.1204
6.710	0.5300	0.0530	1.172	1.7720	0.1772
6.900	0.6300	0.0630	1.362	2.1552	0.2155
7.090	0.6400	0.0640	1.552	2.2201	0.2220
7.270	0.6400	0.0640	1.732	2.2267	0.2227
7.460	0.6300	0.0630	1.922	2.1791	0.2179
7.650	0.6300	0.0630	2.112	2.1523	0.2152
7.830	0.6400	0.0640	2.292	2.1535	0.2153
8.020	0.6500	0.0650	2.482	2.1487	0.2149
8.210	0.6400	0.0640	2.672	2.0779	0.2078
8.400	0.6100	0.0610	2.862	1.9465	0.1947
8.580	0.6400	0.0640	3.042	2.0111	0.2011
8.770	0.6600	0.0660	3.232	2.0433	0.2043
8.950	0.6000	0.0600	3.412	1.8337	0.1834
9.140	0.6200	0.0620	3.602	1.8713	0.1871
9.330	0.6000	0.0600	3.792	1.7905	0.1790
9.510	0.6300	0.0630	3.972	1.8617	0.1862
9.700	0.5900	0.0590	4.162	1.7272	0.1727
9.890	0.7000	0.0700	4.352	2.0316	0.2032
10.070	0.7000	0.0700	4.532	2.0161	0.2016

TABLE VIII: (Continued).

E_x	$P_{(t,pf)}(E_x)$		E_n	$\sigma_{(n,f)}(E_n)$	
(MeV)	Value	Unc.	(MeV)	Value (b)	Unc. (b)
10.260	0.6500	0.0650	4.722	1.8594	0.1859
10.440	0.6500	0.0650	4.902	1.8508	0.1851
10.630	0.6200	0.0620	5.092	1.7604	0.1760
10.810	0.6200	0.0620	5.272	1.7584	0.1758
11.000	0.6200	0.0620	5.462	1.7585	0.1759
11.180	0.6100	0.0610	5.642	1.7318	0.1732
11.370	0.6200	0.0620	5.832	1.7631	0.1763

TABLE IX: Measured ^{242}Pu(^{3}He, df) fission probabilities and the corresponding deduced ^{242}Am(n, f) cross section. A $\pm 10\%$ uncertainty associated with the fission probability data is quoted and reflected in the uncertainty on the deduced $\sigma_{(n,f)}$ values (in barns).

E_x	$P_{(t,pf)}(E_x)$		E_n	$\sigma_{(n,f)}(E_n)$	
(MeV)	Value	Unc.	(MeV)	Value (b)	Unc. (b)
5.260	0.0600	0.0060			
5.450	0.1400	0.0140			
5.640	0.3200	0.0320			
5.840	0.6200	0.0620			
6.030	0.8000	0.0800			
6.220	0.9300	0.0930			
6.410	0.8400	0.0840			
6.600	0.8600	0.0860	0.233	2.8220	0.2822
6.800	0.7600	0.0760	0.433	2.4048	0.2405
6.990	0.6900	0.0690	0.623	2.1737	0.2174
7.180	0.6700	0.0670	0.813	2.1289	0.2129
7.370	0.6000	0.0600	1.003	1.9483	0.1948
7.560	0.5700	0.0570	1.193	1.9004	0.1900
7.750	0.5600	0.0560	1.383	1.9098	0.1910
7.940	0.5700	0.0570	1.573	1.9712	0.1971
8.130	0.5800	0.0580	1.763	2.0124	0.2012
8.320	0.5700	0.0570	1.953	1.9663	0.1966
8.510	0.5700	0.0570	2.143	1.9427	0.1943
8.700	0.5900	0.0590	2.333	1.9793	0.1979
8.890	0.5700	0.0570	2.523	1.8790	0.1879
9.080	0.5800	0.0580	2.713	1.8785	0.1879
9.270	0.5700	0.0570	2.903	1.8150	0.1815

TABLE IX: (Continued).

E_x	$P_{(t,pf)}(E_x)$		E_n	$\sigma_{(n,f)}(E_n)$	
(MeV)	Value	Unc.	(MeV)	Value (b)	Unc. (b)
9.460	0.5800	0.0580	3.093	1.8178	0.1818
9.650	0.5800	0.0580	3.283	1.7915	0.1792
9.840	0.5900	0.0590	3.473	1.7983	0.1798
10.030	0.5900	0.0590	3.663	1.7766	0.1777
10.210	0.5900	0.0590	3.843	1.7579	0.1758
10.400	0.5900	0.0590	4.033	1.7402	0.1740
10.590	0.5900	0.0590	4.223	1.7243	0.1724
10.780	0.6000	0.0600	4.413	1.7388	0.1739
10.970	0.6000	0.0600	4.603	1.7235	0.1724

TABLE X: Measured ^{242}Pu(^{3}He, df) fission probabilities and the corresponding deduced ^{242m}Am(n, f) cross section. A $\pm 10\%$ uncertainty associated with the fission probability data is quoted and reflected in the uncertainty on the deduced $\sigma_{(n,f)}$ values (in barns).

E_x	$P_{(t,pf)}(E_x)$		E_n	$\sigma_{(n,f)}(E_n)$	
(MeV)	Value	Unc.	(MeV)	Value (b)	Unc. (b)
5.260	0.0600	0.0060			
5.450	0.1400	0.0140			
5.640	0.3200	0.0320			
5.840	0.6200	0.0620			
6.030	0.8000	0.0800			
6.220	0.9300	0.0930			
6.410	0.8400	0.0840			
6.600	0.8600	0.0860	0.233	3.1607	0.3161
6.800	0.7600	0.0760	0.433	2.8311	0.2831
6.990	0.6900	0.0690	0.623	2.5976	0.2598
7.180	0.6700	0.0670	0.813	2.4555	0.2456
7.370	0.6000	0.0600	1.003	2.1451	0.2145
7.560	0.5700	0.0570	1.193	2.0237	0.2024
7.750	0.5600	0.0560	1.383	1.9857	0.1986
7.940	0.5700	0.0570	1.573	2.0151	0.2015
8.130	0.5800	0.0580	1.763	2.0309	0.2031
8.320	0.5700	0.0570	1.953	1.9649	0.1965
8.510	0.5700	0.0570	2.143	1.9278	0.1928
8.700	0.5900	0.0590	2.333	1.9568	0.1957
8.890	0.5700	0.0570	2.523	1.8552	0.1855
9.080	0.5800	0.0580	2.713	1.8542	0.1854
9.270	0.5700	0.0570	2.903	1.7913	0.1791

TABLE X: (Continued).

E_x	$P_{(t,pf)}(E_x)$		E_n	$\sigma_{(n,f)}(E_n)$	
(MeV)	Value	Unc.	(MeV)	Value (b)	Unc. (b)
9.460	0.5800	0.0580	3.093	1.7938	0.1794
9.650	0.5800	0.0580	3.283	1.7676	0.1768
9.840	0.5900	0.0590	3.473	1.7744	0.1774
10.030	0.5900	0.0590	3.663	1.7533	0.1753
10.210	0.5900	0.0590	3.843	1.7352	0.1735
10.400	0.5900	0.0590	4.033	1.7181	0.1718
10.590	0.5900	0.0590	4.223	1.7021	0.1702
10.780	0.6000	0.0600	4.413	1.7154	0.1715
10.970	0.6000	0.0600	4.603	1.7003	0.1700

TABLE XI: Measured ^{244}Pu(^{3}He, tf) fission probabilities and the corresponding deduced ^{243}Am(n, f) cross section. A $\pm 10\%$ uncertainty associated with the fission probability data is quoted and reflected in the uncertainty on the deduced $\sigma_{(n,f)}$ values (in barns).

E_x	$P_{(t,pf)}(E_x)$		E_n	$\sigma_{(n,f)}(E_n)$	
(MeV)	Value	Unc.	(MeV)	Value (b)	Unc. (b)
6.030	0.0500	0.0050	0.666	0.1442	0.0144
6.190	0.1500	0.0150	0.826	0.4591	0.0459
6.360	0.2300	0.0230	0.996	0.7389	0.0739
6.530	0.3600	0.0360	1.166	1.1939	0.1194
6.700	0.3800	0.0380	1.336	1.2895	0.1289
6.870	0.4100	0.0410	1.506	1.4138	0.1414
7.040	0.4300	0.0430	1.676	1.4926	0.1493
7.210	0.3900	0.0390	1.846	1.3512	0.1351
7.370	0.3700	0.0370	2.006	1.2720	0.1272
7.540	0.3900	0.0390	2.176	1.3242	0.1324
7.710	0.3700	0.0370	2.346	1.2375	0.1238
7.880	0.3700	0.0370	2.516	1.2177	0.1218
8.050	0.3700	0.0370	2.686	1.1981	0.1198
8.220	0.4000	0.0400	2.856	1.2751	0.1275
8.390	0.4400	0.0440	3.026	1.3821	0.1382
8.560	0.4300	0.0430	3.196	1.3323	0.1332
8.720	0.3600	0.0360	3.356	1.1022	0.1102
8.890	0.3800	0.0380	3.526	1.1499	0.1150
9.060	0.3500	0.0350	3.696	1.0477	0.1048
9.230	0.3600	0.0360	3.866	1.0670	0.1067
9.400	0.3800	0.0380	4.036	1.1161	0.1116
9.570	0.3200	0.0320	4.206	0.9321	0.0932

TABLE XI: (Continued).

E_x	$P_{(t,pf)}(E_x)$		E_n	$\sigma_{(n,f)}(E_n)$	
(MeV)	Value	Unc.	(MeV)	Value (b)	Unc. (b)
9.740	0.3800	0.0380	4.376	1.0982	0.1098
9.910	0.3500	0.0350	4.546	1.0042	0.1004
10.070	0.3700	0.0370	4.706	1.0553	0.1055
10.240	0.3600	0.0360	4.876	1.0219	0.1022
10.410	0.4300	0.0430	5.046	1.2169	0.1217
10.580	0.4000	0.0400	5.216	1.1301	0.1130
10.750	0.3600	0.0360	5.386	1.0166	0.1017
10.920	0.3700	0.0370	5.556	1.0452	0.1045
11.090	0.3500	0.0350	5.726	0.9898	0.0990
11.260	0.3900	0.0390	5.896	1.1045	0.1105
11.420	0.3600	0.0360	6.056	1.0214	0.1021
11.590	0.3600	0.0360	6.226	1.0235	0.1024
11.760	0.3700	0.0370	6.396	1.0544	0.1054
11.930	0.4000	0.0400	6.566	1.1427	0.1143
12.100	0.4000	0.0400	6.736	1.1456	0.1146
12.270	0.3800	0.0380	6.906	1.0911	0.1091
12.440	0.4100	0.0410	7.076	1.1801	0.1180
12.610	0.3700	0.0370	7.246	1.0674	0.1067
12.770	0.4100	0.0410	7.406	1.1852	0.1185
12.940	0.4100	0.0410	7.576	1.1877	0.1188
13.110	0.3600	0.0360	7.746	1.0447	0.1045

TABLE XII: Measured ^{244}Pu(^{3}He, df) fission probabilities and the corresponding deduced ^{244}Am(n, f) cross section. A ±10% uncertainty associated with the fission probability data is quoted and reflected in the uncertainty on the deduced $\sigma_{(n,f)}$ values (in barns).

E_x	$P_{(t,pf)}(E_x)$		E_n	$\sigma_{(n,f)}(E_n)$	
(MeV)	Value	Unc.	(MeV)	Value (b)	Unc. (b)
5.040	0.0500	0.0050			
5.210	0.1100	0.0110			
5.370	0.2600	0.0260			
5.540	0.4700	0.0470			
5.710	0.6500	0.0650			
5.870	0.7600	0.0760			
6.040	0.7800	0.0780			
6.210	0.7200	0.0720	0.156	2.5918	0.2592
6.380	0.7000	0.0700	0.326	2.8976	0.2898
6.540	0.5900	0.0590	0.486	2.7835	0.2784
6.710	0.5200	0.0520	0.656	2.5828	0.2583
6.880	0.4900	0.0490	0.826	2.3353	0.2335
7.050	0.4100	0.0410	0.996	1.7887	0.1789
7.220	0.3800	0.0380	1.166	1.5546	0.1555
7.390	0.3900	0.0390	1.336	1.5252	0.1525
7.550	0.4000	0.0400	1.496	1.5165	0.1517
7.720	0.3600	0.0360	1.666	1.3279	0.1328
7.890	0.3900	0.0390	1.836	1.4018	0.1402
8.060	0.3800	0.0380	2.006	1.3318	0.1332
8.220	0.3600	0.0360	2.166	1.2328	0.1233
8.390	0.3700	0.0370	2.336	1.2376	0.1238
8.560	0.3700	0.0370	2.506	1.2107	0.1211

TABLE XII: (Continued).

E_x	$P_{(t,pf)}(E_x)$		E_n	$\sigma_{(n,f)}(E_n)$	
(MeV)	Value	Unc.	(MeV)	Value (b)	Unc. (b)
8.730	0.3800	0.0380	2.676	1.2185	0.1218
8.890	0.3700	0.0370	2.836	1.1659	0.1166
9.060	0.3700	0.0370	3.006	1.1464	0.1146
9.230	0.3700	0.0370	3.176	1.1291	0.1129
9.400	0.3700	0.0370	3.346	1.1137	0.1114
9.560	0.3800	0.0380	3.506	1.1305	0.1131
9.760	0.3700	0.0370	3.706	1.0863	0.1086
9.930	0.4000	0.0400	3.876	1.1624	0.1162
10.100	0.3800	0.0380	4.046	1.0941	0.1094
10.260	0.3800	0.0380	4.206	1.0855	0.1085
10.430	0.3800	0.0380	4.376	1.0770	0.1077
10.600	0.4000	0.0400	4.546	1.1254	0.1125
10.770	0.3800	0.0380	4.716	1.0625	0.1062
10.930	0.3600	0.0360	4.876	1.0022	0.1002
11.100	0.4000	0.0400	5.046	1.1103	0.1110

TABLE XIII: Measured ^{244}Pu(^{3}He, df) fission probabilities and the corresponding deduced ^{244m}Am(n, f) cross section. A $\pm 10\%$ uncertainty associated with the fission probability data is quoted and reflected in the uncertainty on the deduced $\sigma_{(n,f)}$ values (in barns).

E_x	$P_{(t,pf)}(E_x)$		E_n	$\sigma_{(n,f)}(E_n)$	
(MeV)	Value	Unc.	(MeV)	Value (b)	Unc. (b)
5.040	0.0500	0.0050			
5.210	0.1100	0.0110			
5.370	0.2600	0.0260			
5.540	0.4700	0.0470			
5.710	0.6500	0.0650			
5.870	0.7600	0.0760			
6.040	0.7800	0.0780			
6.210	0.7200	0.0720	0.156	2.1780	0.2178
6.380	0.7000	0.0700	0.326	2.0379	0.2038
6.540	0.5900	0.0590	0.486	1.7117	0.1712
6.710	0.5200	0.0520	0.656	1.5720	0.1572
6.880	0.4900	0.0490	0.826	1.5168	0.1517
7.050	0.4100	0.0410	0.996	1.3111	0.1311
7.220	0.3800	0.0380	1.166	1.2532	0.1253
7.390	0.3900	0.0390	1.336	1.3200	0.1320
7.550	0.4000	0.0400	1.496	1.3766	0.1377
7.720	0.3600	0.0360	1.666	1.2481	0.1248
7.890	0.3900	0.0390	1.836	1.3486	0.1349
8.060	0.3800	0.0380	2.006	1.3011	0.1301
8.220	0.3600	0.0360	2.166	1.2173	0.1217
8.390	0.3700	0.0370	2.336	1.2336	0.1234
8.560	0.3700	0.0370	2.506	1.2166	0.1217

TABLE XIII: (Continued).

E_x	$P_{(t,pf)}(E_x)$		E_n	$\sigma_{(n,f)}(E_n)$	
(MeV)	Value	Unc.	(MeV)	Value (b)	Unc. (b)
8.730	0.3800	0.0380	2.676	1.2325	0.1233
8.890	0.3700	0.0370	2.836	1.1848	0.1185
9.060	0.3700	0.0370	3.006	1.1690	0.1169
9.230	0.3700	0.0370	3.176	1.1540	0.1154
9.400	0.3700	0.0370	3.346	1.1402	0.1140
9.560	0.3800	0.0380	3.506	1.1589	0.1159
9.760	0.3700	0.0370	3.706	1.1153	0.1115
9.930	0.4000	0.0400	3.876	1.1949	0.1195
10.100	0.3800	0.0380	4.046	1.1258	0.1126
10.260	0.3800	0.0380	4.206	1.1172	0.1117
10.430	0.3800	0.0380	4.376	1.1080	0.1108
10.600	0.4000	0.0400	4.546	1.1572	0.1157
10.770	0.3800	0.0380	4.716	1.0925	0.1092
10.930	0.3600	0.0360	4.876	1.0302	0.1030
11.100	0.4000	0.0400	5.046	1.1433	0.1143

[1] W. Younes and H. C. Britt, Tech. Rep. UCRL-ID-154206, LLNL (2003).

[2] J. D. Cramer and H. C. Britt, Phys. Rev. C **2**, 2350 (1970).

[3] A. Gavron, H. C. Britt, E. Konecny, J. Weber, and J. B. Wilhelmy, Phys. Rev. C **13**, 2374 (1976).

[4] H. C. Britt and J. B. Wilhelmy, Nucl. Sci. Eng. **72**, 222 (1979).

[5] F. S. Dietrich, private communication.

[6] W. Younes and H. C. Britt, Phys. Rev. C **67**, 024610 (2003).

[7] W. Younes and H. C. Britt, Phys. Rev. C **68**, 034610 (2003).

[8] J. D. Cramer and H. C. Britt, Nucl. Sci. and Eng. **41**, 177 (1970).

[9] H. C. Britt, M. Bolsterli, J. R. Nix, and J. L. Norton, Phys. Rev. C **7**, 801 (1973).

[10] H. C. Britt, in *Proceedings of the Symposium on Physics and Chemistry of Fission* (International Atomic Energy Agency, Vienna, 1979), vol. 1, p. 3.

[11] Cross Section Evaluation Working Group, *ENDF/B-VI Summary Documentation,* Report **BNL-NCS-17541 (ENDF-201)** (1991), edited by P. F. Rose, National Nuclear Data Center, Brookhave Laboratory, Upton, NY, USA.

[12] *Evaluated neutron data library*, www-ndg.llnl.gov.

[13] J. C. Browne, R. M. White, R. E. Howe, R. J. Dougan, R. J. Dupzyk, and J. H. Landrum, Phys. Rev. C **29**, 2188 (1984).

[14] B. I. Fursov, B. F. Samylin, V. S. Shorin, S. A. Badikov, M. I. Svirin, E. Y. Baranov, E. S. Lavrov, V. I. Mil'shin, V. B. Pavlovich, S. V. Pupko, et al., in *International Conference on Nuclear Data for Science and Technology* (Italian Physical Society, Bologna, Italy, 1997), vol. 1, p. 488.

[15] B. I. Fursov, E. J. Baranov, M. P. Klemyshev, B. F. Samylin, G. N. Smirenkin, and Y. M. Turchin, Atomnaya Energiya **59**, 339 (1985).

[16] H. Terayama, Y. Karino, F. Manabe, M. Yanagawa, K. Kanda, and N. Hirakawa, Tech. Rep. NETU-47, Tohoku University, Sendai, Japan (1986).

[17] K. Kanda, H. Imaruoka, H. Terayama, Y. Karino, and H. N, J. Nucl. Sci. and Tech. **24**, 423 (1987).

[18] H. Knitter and C. Budtz-Jorgensen, Nucl. Sci. and Eng. **99**, 1 (1988).

[19] A. A. Goverdovskiy, A. K. Gordyushin, B. D. Kuz'minov, V. F. Mitrofanov, A. I. Sergachev, S. M. Solov'ev, and T. E. Kuz'mina, Atomnaya Energiya **67**, 30 (1989).

[20] J. W. Behrens and J. C. Browne, Nucl. Sci. and Eng. **77**, 444 (1981).

[21] J. W. Behrens, J. C. Browne, and J. C. Walden, Nucl. Sci. and Eng. **80**, 393 (1982).

[22] J. W. Meadows, Nucl. Sci. and Eng. **85**, 271 (1983).

[23] J. W. T. Dabbs, C. H. Johnson, and C. E. B. Jr, Nucl. Sci. and Eng. **83**, 22 (1983).

[24] J. W. T. Dabbs, C. E. B. Jr, S. Raman, R. J. Dougan, and R. W. Hoff, Nucl. Sci. and Eng. **84**, 1 (1983).

TABLE XIV: Relevant properties of the isotopes studied in this paper.

Neutron target	J^π	$T_{1/2}$	E_x (keV)
^{236}Np	6^-	1.54×10^5 yr	0
^{236m}Np	1^a	22.5 h	60
^{237}Np	$5/2^+$	2.144×10^6 yr	0
^{238}Np	2^+	2.117 days	0
^{237}Pu	$7/2^-$	45.2 days	0
^{237m}Pu	$1/2^+$	0.18 s	145.5
^{240}Am	3^-	50.8 h	0
^{241}Am	$5/2^-$	432.2 yr	0
^{242}Am	1^-	16.02 h	0
^{242m}Am	5^-	141 yr	48.6
^{243}Am	$5/2^-$	7370 yr	0
^{244}Am	6^-	10.1 h	0
^{244m}Am	1^+	$\approx$ 26 min	86.1

[a]Parity unknown, positive parity assumed in the calculations.

TABLE XV: Ratio R of the average surrogate-to-measured (n, f) cross sections for the range 1 $\leq E_n$ (MeV) $\leq$ 6.

Neutron target	R
^{237}Np	1.03
^{241}Am	1.09
^{242m}Am	1.09
^{243}Am	0.83

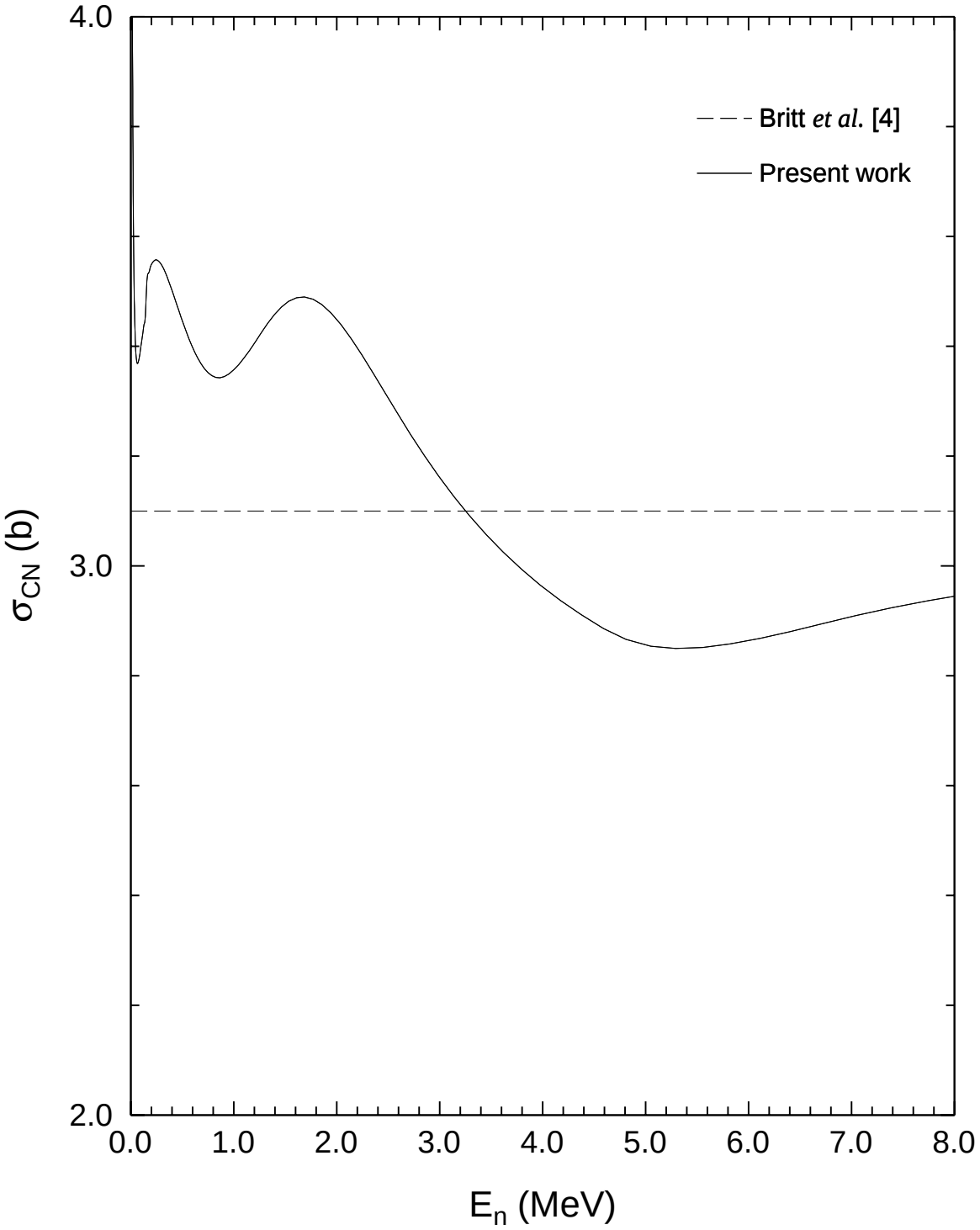

FIG. 1: Calculated neutron compound cross sections. Note the offset zero.

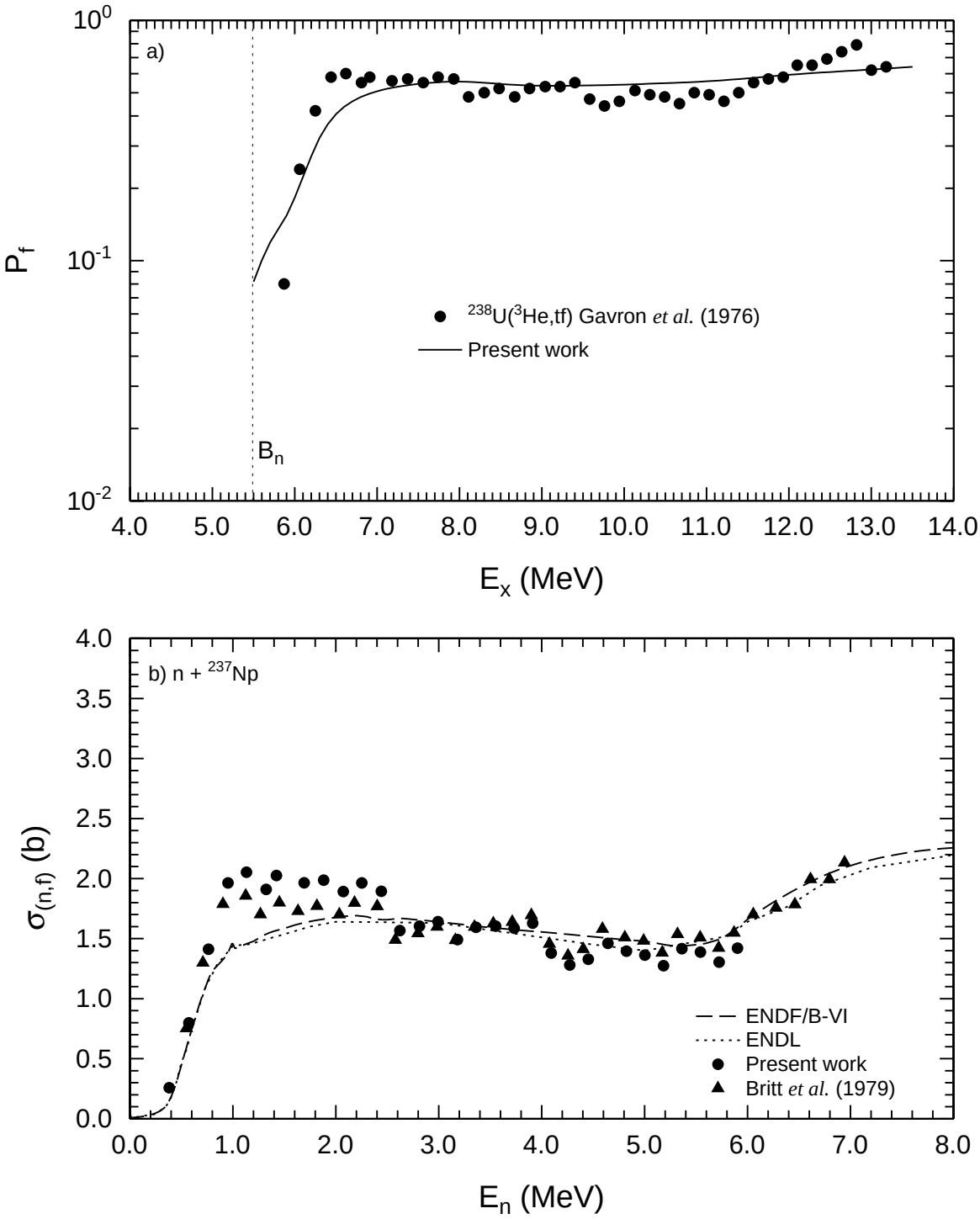

FIG. 2: Estimated ^{237}Np(n, f) cross section. Panel a) shows the best fit to ^{238}U(^{3}He$, tf)$ fission-probability data [3]. The neutron binding energy $B_n = 5.488$ MeV is denoted by a vertical dotted line. Panel b) shows the deduced (n, f) cross section, compared to ENDF/B-VI [11] and ENDL [12] evaluations, and the estimates of Britt *et al.* [4].

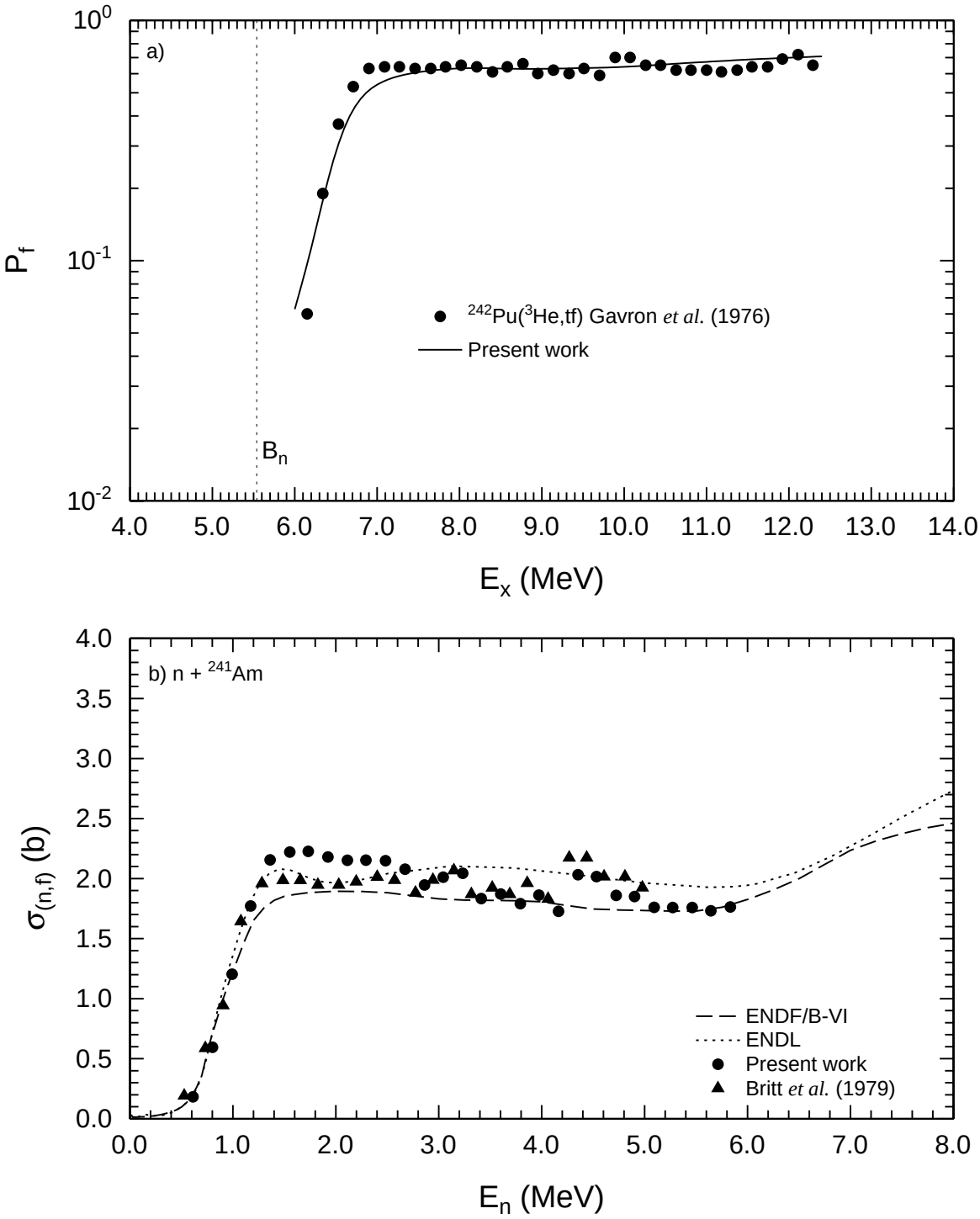

FIG. 3: Estimated ^{241}Am(n, f) cross section. Panel a) shows the best fit to ^{242}Pu(^{3}He$, tf)$ fission-probability data [3]. The neutron binding energy $B_n = 5.538$ MeV is denoted by a vertical dotted line. Panel b) shows the deduced (n, f) cross section, compared to ENDF/B-VI [11] and ENDL [12] evaluations, and the estimates of Britt *et al.* [4].

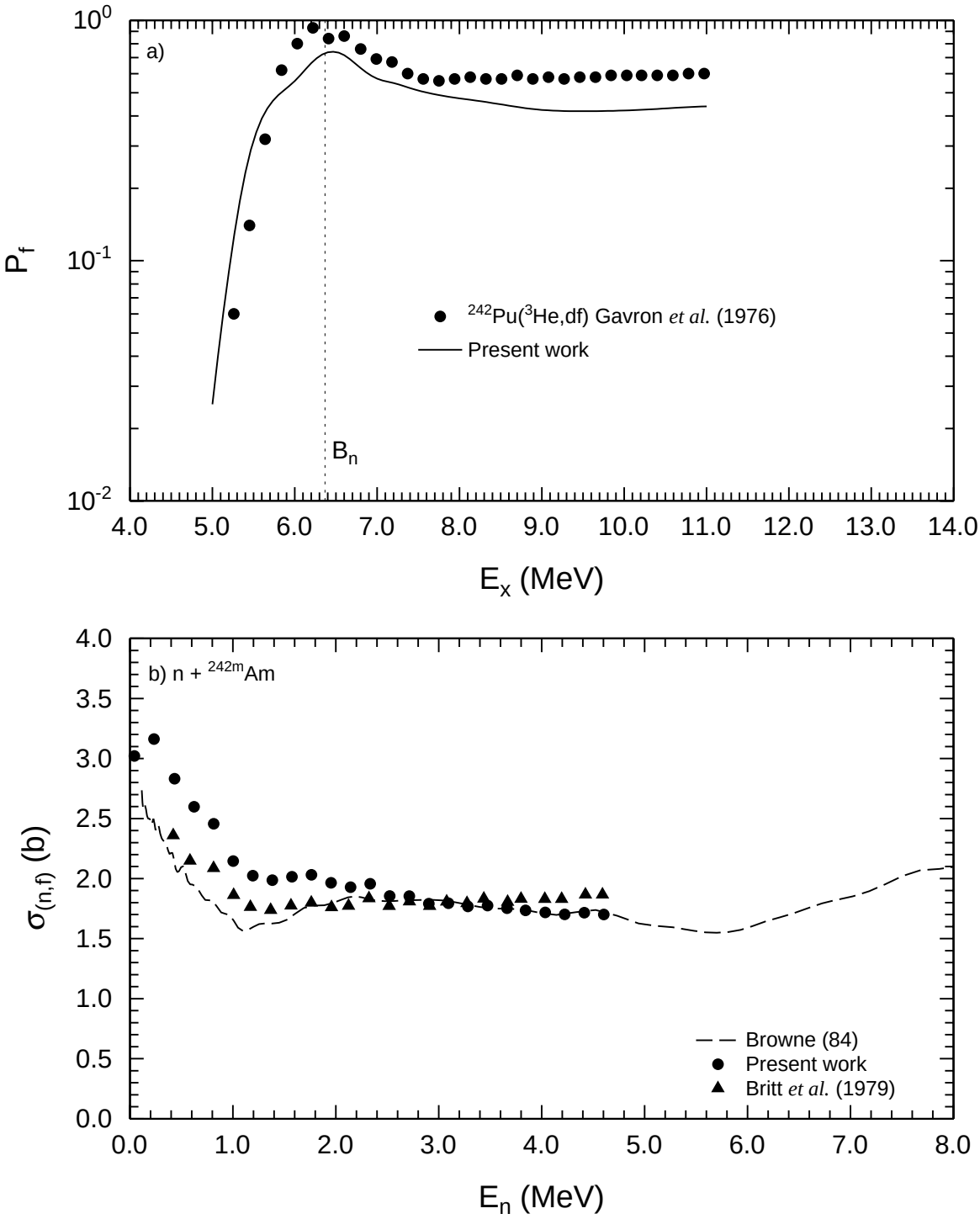

FIG. 4: Estimated ^{242m}Am(n, f) cross section. Panel a) shows the best fit to ^{242}Pu(^{3}He, df) fission-probability data [3]. The neutron binding energy $B_n = 6.367$ MeV is denoted by a vertical dotted line. Panel b) shows the deduced (n, f) cross section, compared to data from Browne *et al.* [13] and the estimates of Britt *et al.* [4].

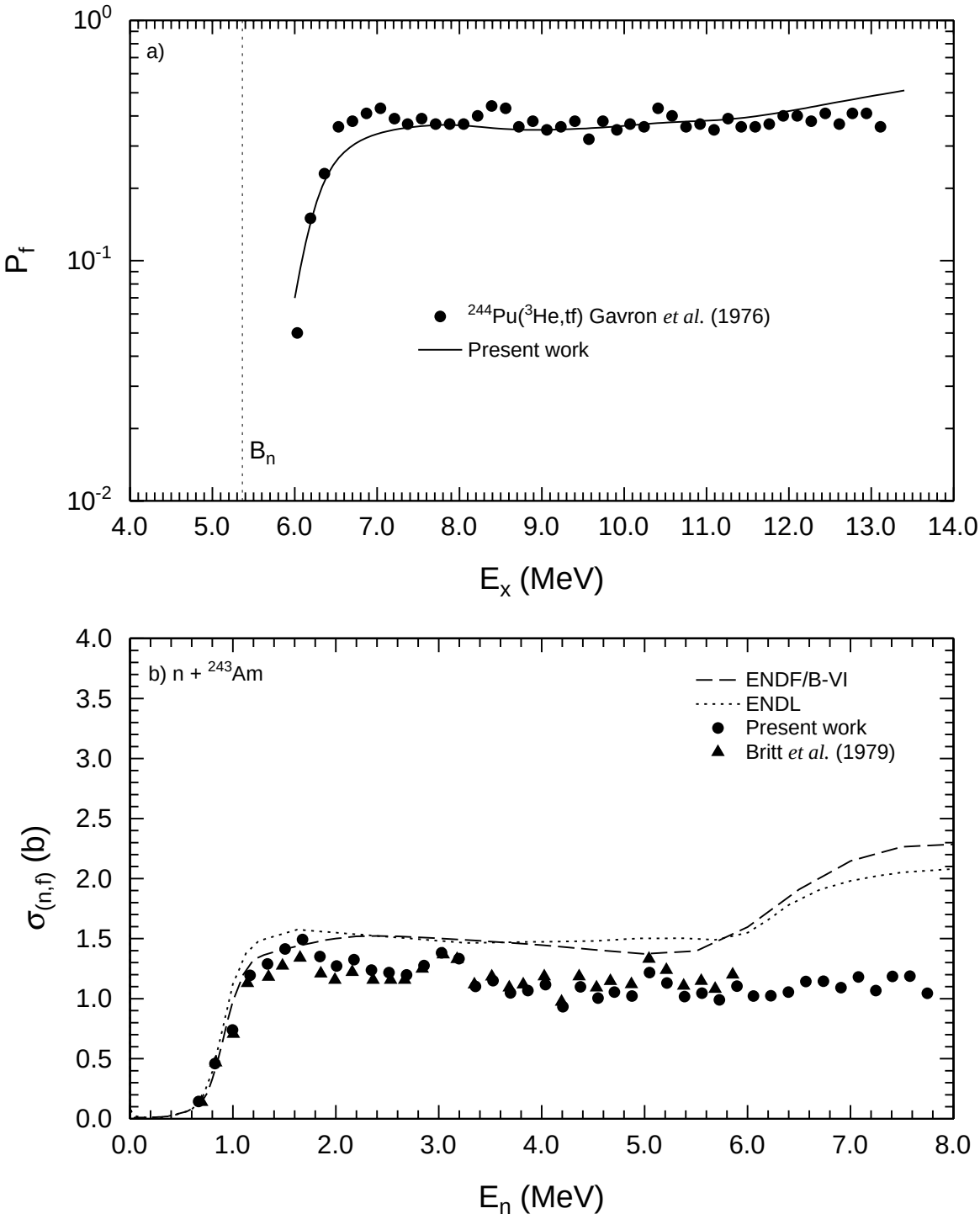

FIG. 5: Estimated ^{243}Am(n,f) cross section. Panel a) shows the best fit to ^{244}Pu(^{3}He$,tf$) fission-probability data [3]. The neutron binding energy $B_n = 5.364$ MeV is denoted by a vertical dotted line. Panel b) shows the deduced (n,f) cross section, compared to ENDF/B-VI [11] and ENDL [12] evaluations, and the estimates of Britt *et al.* [4].

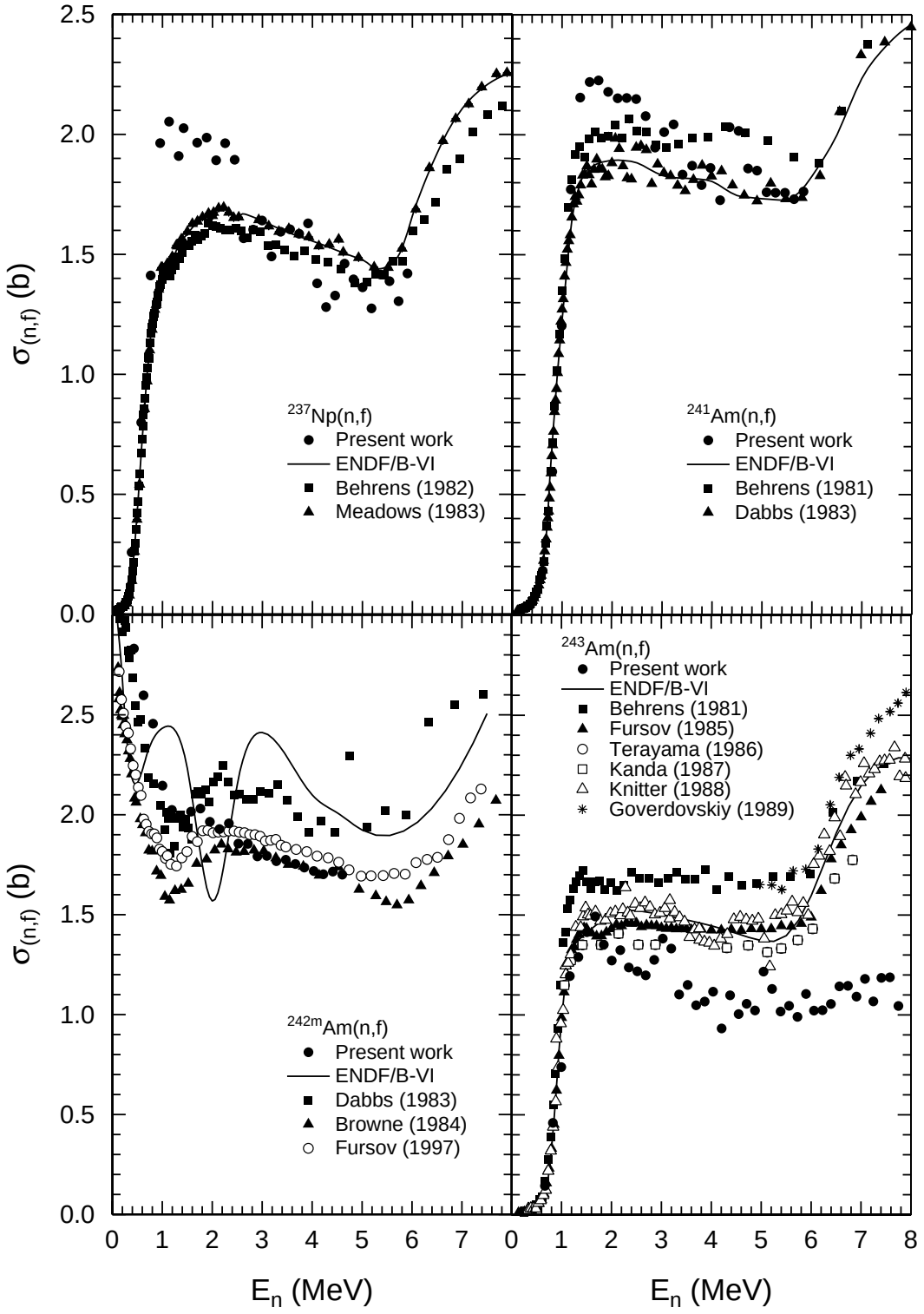

FIG. 6: Comparison of (n, f) cross sections from the present work and ENDF/B-VI [11] evaluations to experimental measurements of the (n, f) reaction on targets of ^{237}Np [21, 22], ^{241}Am [20, 23], ^{242m}Am [13, 14, 24], and ^{243}Am [15–20].

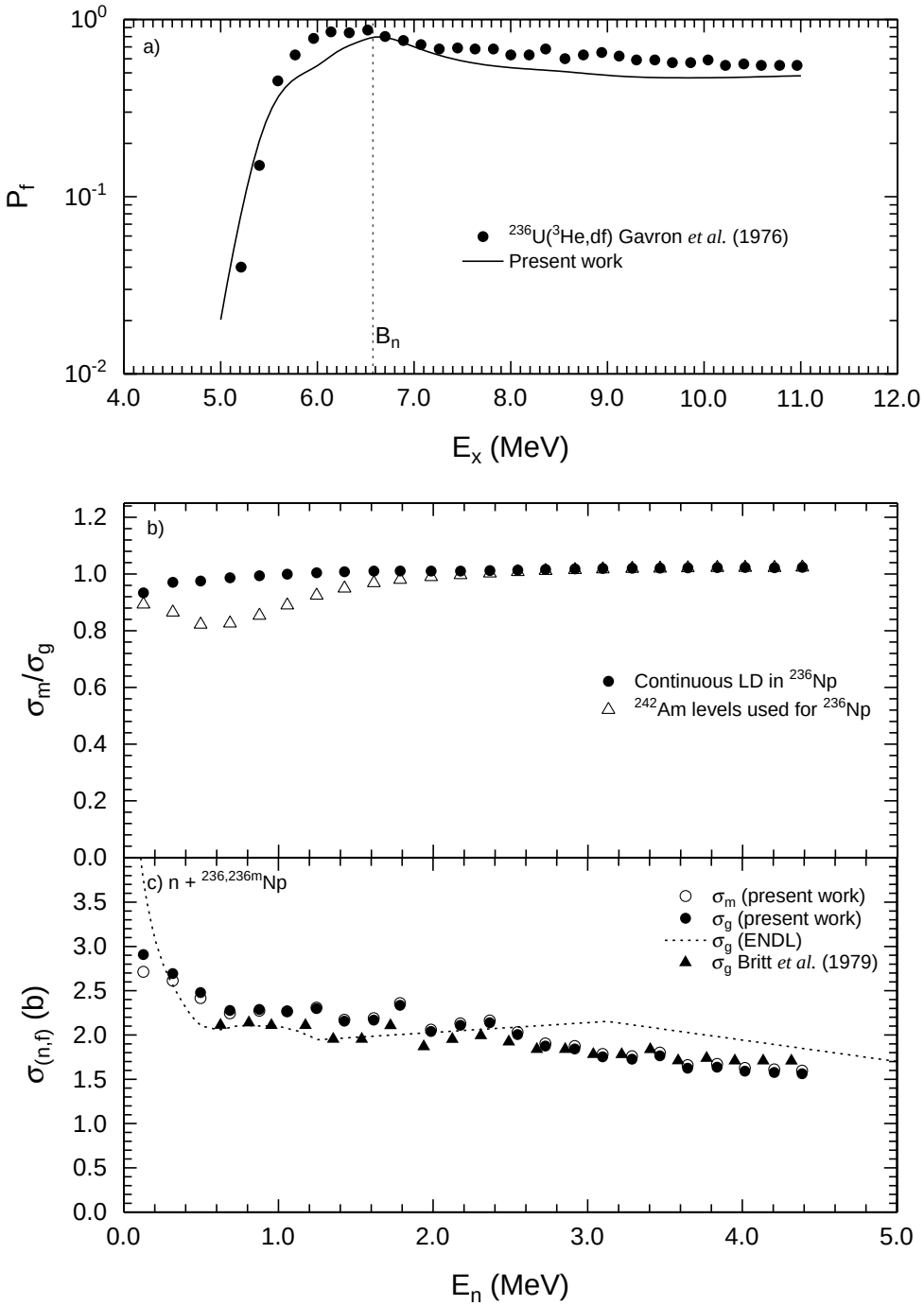

FIG. 7: Estimated ^{236m}Np(n, f) cross section. Panel a) shows the best fit to ^{236}U(^{3}He, df) fission-probability data [3]. The neutron binding energy $B_n = 6.574$ MeV is denoted by a vertical dotted line. Panel b) shows the deduced isomer-to-ground-state fission ratio, compared to a test calculation where the known ^{242}Am discrete states are used in the first well of the neutron-out residual nucleus, ^{236}Np. Panel c) shows the individual ground-state and isomer (n, f) cross sections, compared to the ground-state cross sections from the ENDL [12] evaluation and the estimates of Britt *et al.* [4].

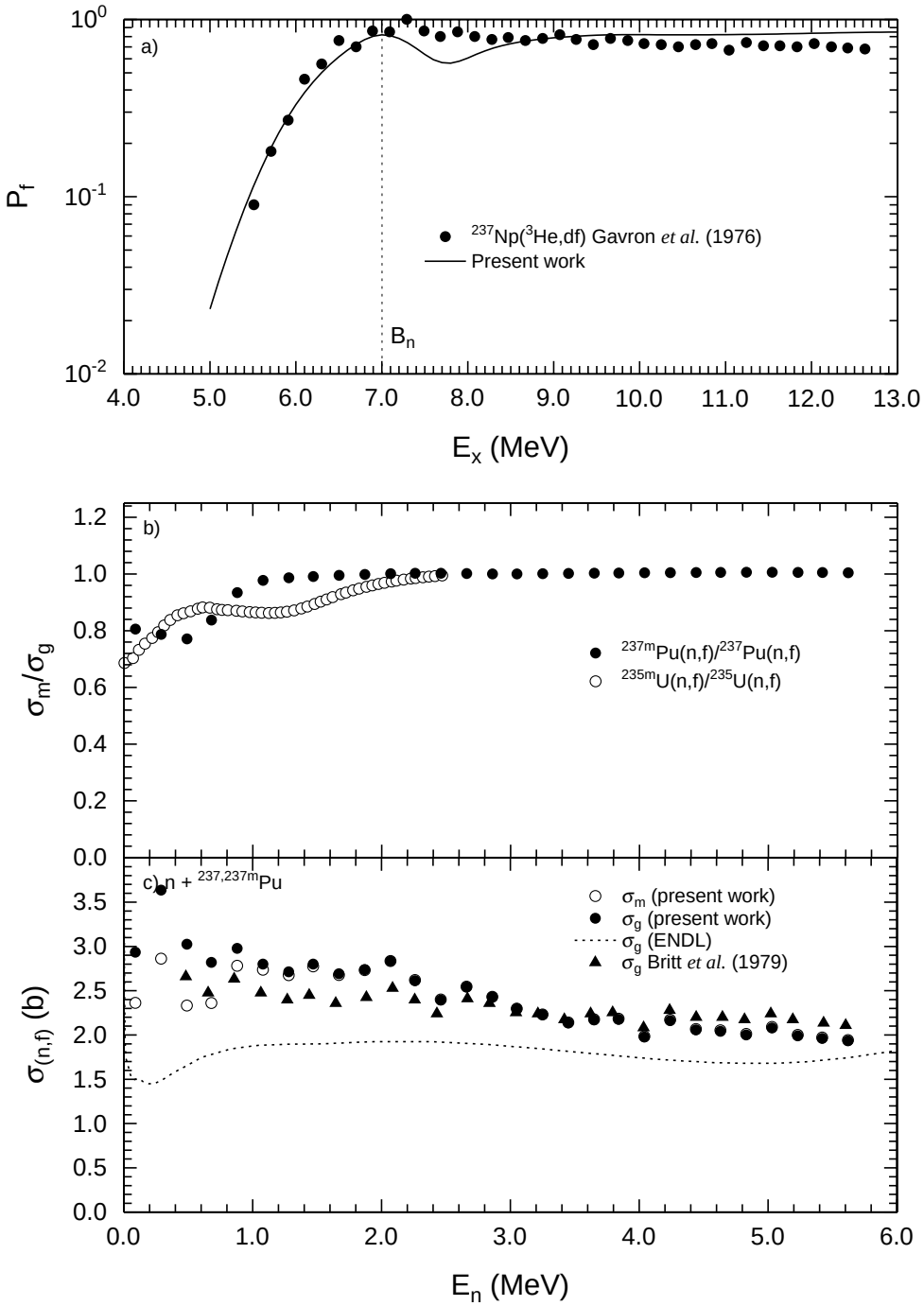

FIG. 8: Estimated ^{237m}Pu(n, f) cross section. Panel a) shows the best fit to ^{237}Np$(^3$He$, df)$ fission-probability data [3]. The neutron binding energy $B_n = 7.001$ MeV is denoted by a vertical dotted line. Panel b) shows the deduced isomer-to-ground-state ratio, compared to the same ratio for a ^{235}U target. Panel c) shows the individual ground-state and isomer (n, f) cross sections, compared to the ground-state cross sections from the ENDL [12] evaluation and the estimates of Britt *et al.* [4].

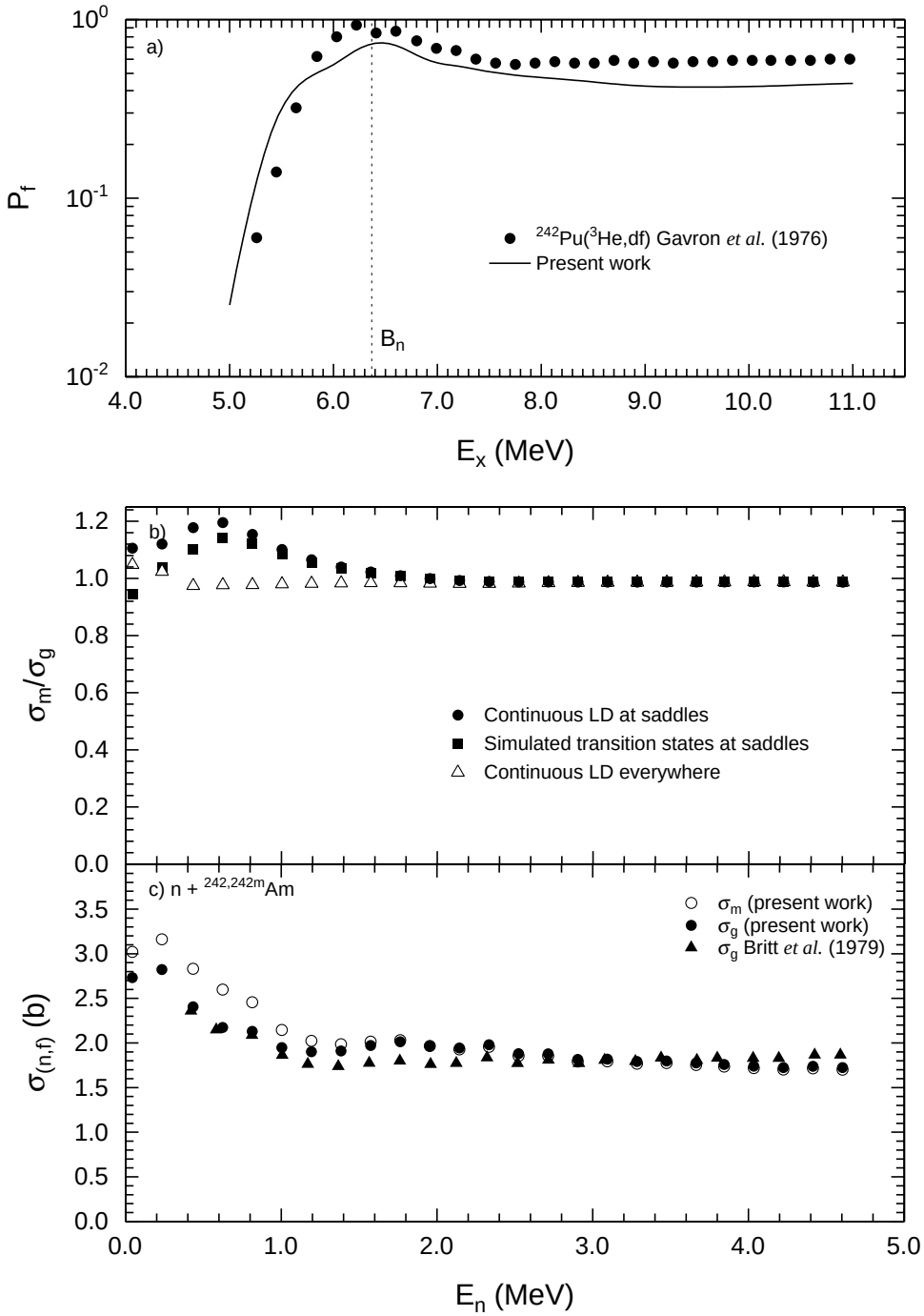

FIG. 9: Estimated ^{242m}Am(n, f) cross section. Panel a) shows the best fit to ^{242}Pu(^{3}He, df) fission-probability data [3]. The neutron binding energy $B_n = 6.367$ MeV is denoted by a vertical dotted line. Panel b) shows the deduced isomer-to-ground-state ratio, compared to test calculations where (i) discrete states are used at the fission saddles, and (ii) all discrete states in the model are replaced by continuous level densities. Panel c) shows the individual ground-state and isomer (n, f) cross sections, compared to the ground-state cross section estimated by Britt *et al.* [4].

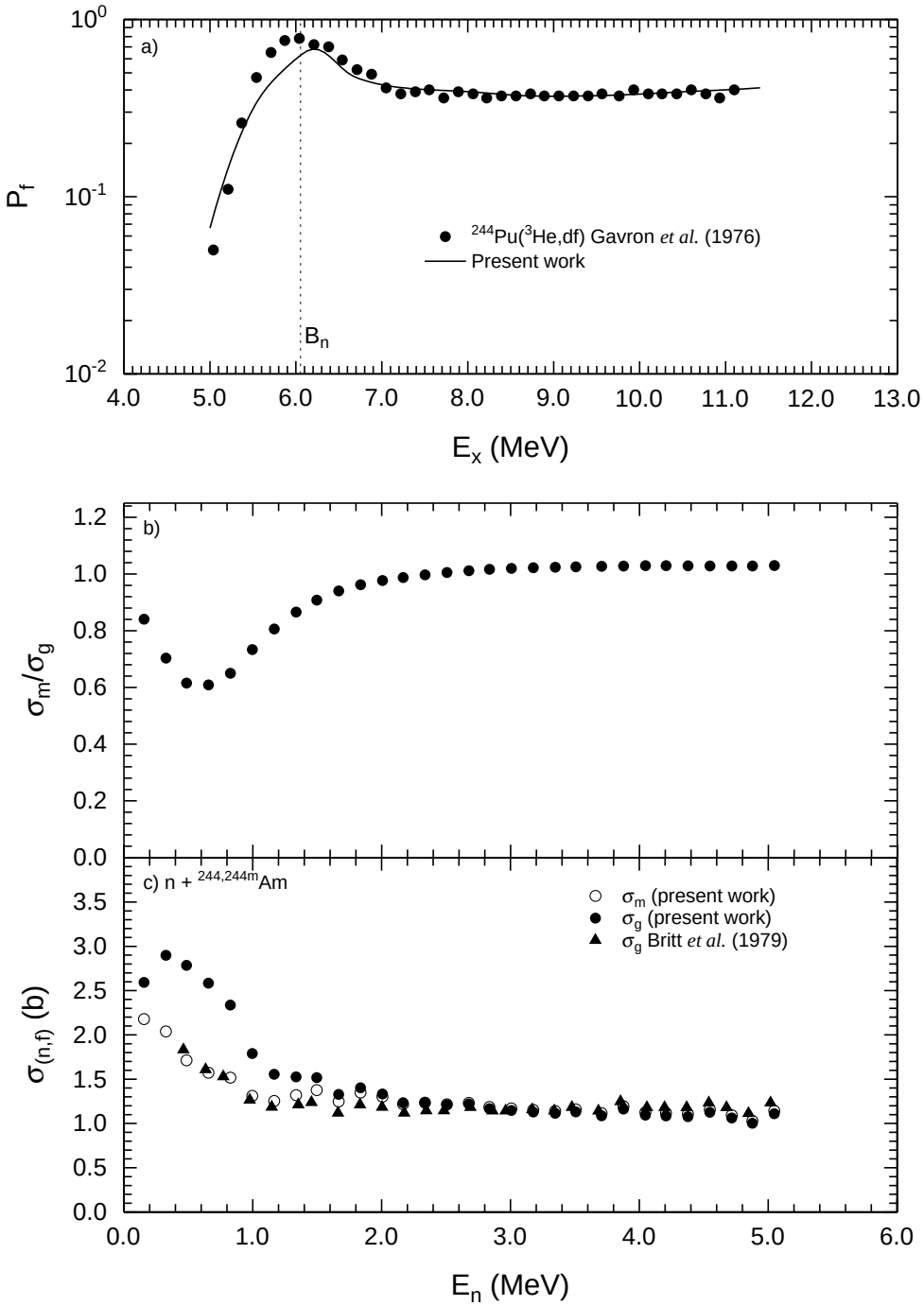

FIG. 10: Estimated ^{244m}Am(n, f) cross section. Panel a) shows the best fit to ^{244}Pu(^{3}He, df) fission-probability data [3]. The neutron binding energy $B_n = 6.054$ MeV is denoted by a vertical dotted line. Panel b) shows the deduced isomer-to-ground-state ratio. Panel c) shows the individual ground-state and isomer (n, f) cross sections, compared to the ground-state cross section estimated by Britt *et al.* [4].

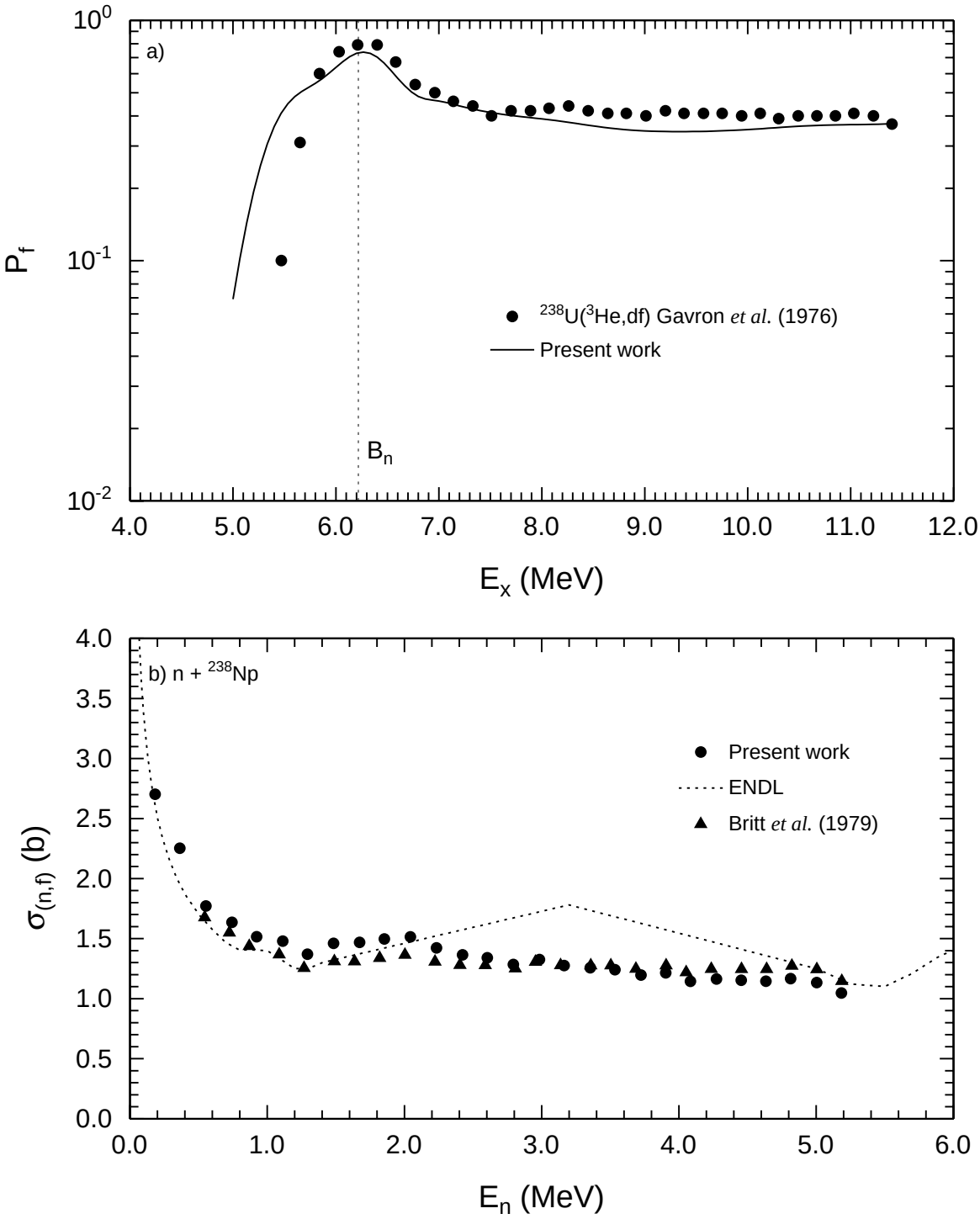

FIG. 11: Estimated ^{238}Np(n, f) cross section. Panel a) shows the best fit to ^{238}U(^{3}He, df) fission-probability data [3]. The neutron binding energy $B_n = 6.217$ MeV is denoted by a vertical dotted line. Panel b) shows the deduced (n, f) cross section, compared to the ENDL [12] evaluation, and the estimates of Britt *et al.* [4].

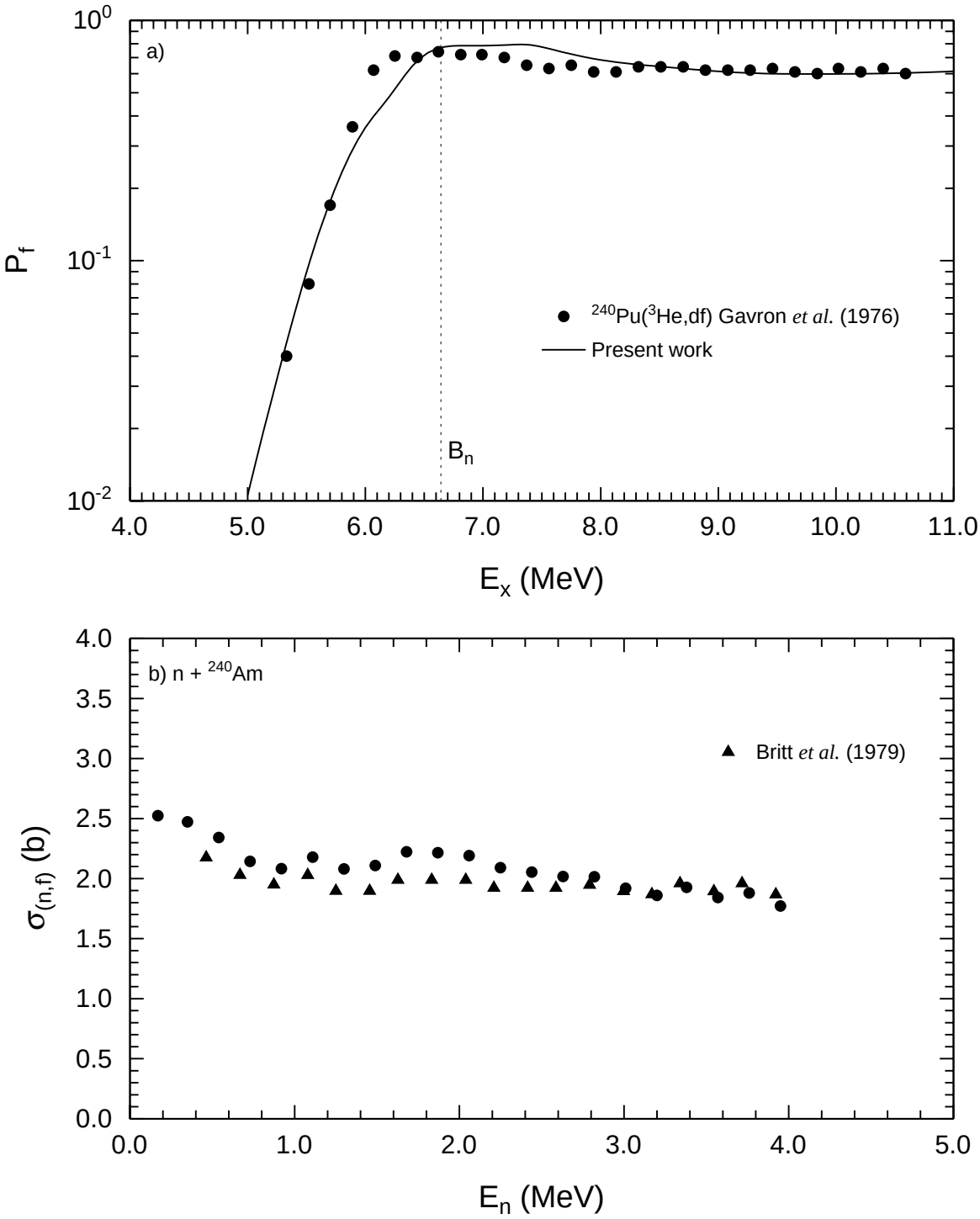

FIG. 12: Estimated ^{240}Am(n, f) cross section. Panel a) shows the best fit to ^{240}Pu(^{3}He, *df*) fission-probability data [3]. The neutron binding energy $B_n = 6.641$ MeV is denoted by a vertical dotted line. Panel b) shows the deduced (n, f) cross section, compared to the estimates of Britt *et al.* [4].